Inorg. Chem. **2004**, *43*, 5833–5849

Sulfur Bridging Interactions of Cis-Planar Ni^{II}–S_2N_2 Coordination Units with Nickel(II), Copper(I,II), Zinc(II), and Mercury(II): A Library of Bridging Modes, Including $Ni^{II}(\mu_2\text{-SR})_2M^{I,II}$ Rhombs

P. Venkateswara Rao, Sumit Bhaduri, Jianfeng Jiang, and R. H. Holm*

Department of Chemistry and Chemical Biology, Harvard University, Cambridge, Massachusetts 02138

Received April 8, 2004

Sulfur bridging interactions between three cis-planar Ni^{II}-S_2N_2 complexes and Ni^{II}, $Cu^{I,II}$, Zn^{II}, and Hg^{II} reactants were investigated by synthesis and X-ray crystal structures of some 24 complexes. This work was stimulated by recent crystallographic structures of the A-cluster of carbon monoxide dehydrogenase/acetylcoenzyme A synthase. This bridged biological assembly has the minimal formulation $[Fe_4S_4]$–$(\mu_2\text{-}S_{Cys})$–$[M((\mu_2\text{-}S_{Cys})_2Gly)Ni]$ with M = Ni^{II}, Cu^{I}, and Zn^{II} at sites distal and proximal, respectively, to the iron–sulfur cluster. Bridges supported by representations of the distal nickel site were sought by reactions of the complexes $[Ni^{II}(L_H\text{-}S_2N_2)]^{2-}$ and $[Ni^{II}(L_R\text{-}S_2N_2)]$, with 5–5–5 chelate ring patterns. Reaction products implicate the bridges Ni–$(\mu_2\text{-S})_{1,2}$–M in a variety of molecular structures, some with previously unknown connectivities of bridge atoms. The most frequently encountered bridge units are the nonplanar rhombs $Ni(\mu_2\text{-S})_2M$ involving both sulfur atoms of a given complex. Those with M = Ni^{II} are biologically relevant inasmuch as the catalytic metal at the proximal site is nickel. The complex $[Ni(L\text{-}655)]^{2-}$, containing the 6–5–5 ring pattern and coordination sphere of the distal nickel site, was prepared and structurally characterized. It was shown to sustain $Ni_2(\mu_2\text{-S})_2$ rhombic interactions in the form of trinuclear $[\{Ni(L\text{-}655)\}_2Ni]^{2-}$ and $[\{Ni(L\text{-}655)\}Ni(R_2PCH_2CH_2PR_2)]$ (R = Et, Ph) in which the second Ni^{II} simulates the proximal site. Bridging interactions of Ni^{II}–S_2N_2 complexes are summarized, and geometrical features of $Ni_2(\mu_2\text{-S})_2$ rhombs in these complexes, as dependent on ring patterns, are considered (L_H-S_2N_2 = *N,N′*-ethylenebis(2-mercaptoisobutyramide)(4–); L_R-S_2N_2 = *trans-rac-N,N′*-bis(2-mercapto-2-methylprop-1-yl)-1,2-cyclohexanediamine(2–); L-655 = *N*-(2-mercaptopropyl)-*N′*-(2′-mercaptoethyl)glycinamide(4–)).

Introduction

Bridged biological metal site assemblies, composed of two distinct parts coupled through one or more metal−ligand covalent bridges in a protein structure, propound a substantial synthetic challenge in biomimetic inorganic chemistry.[1,2] Among enzymes incorporating bridged assemblies, carbon monoxide dehydrogenase/acetyl coenzyme A synthase (CODH/ACS)[3−5] is notable in this respect for two clusters, whose structural definition has reached the stage that they are tenable objectives of synthesis. The C-cluster is the site of CO/CO_2 interconversion and is a nickel−iron−sulfur cluster with a $NiFe_4S_{4,5}$ core containing a $NiFe_3S_4$ cuboidal-type fragment to which is bridged an exo iron atom.[6,7] The A-cluster is the site of the synthesis of acetyl-CoA from coenzyme A, carbon monoxide, and a methyl group supplied by a corrinoid protein. Current X-ray structural information on the enzyme(s) from *Moorella thermoacetica* indicates the minimal formulation $[Fe_4S_4]-(\mu_2\text{-}S_{Cys})-[M((\mu_2\text{-}S_{Cys})_2Gly)\text{-}Ni]$ with M = Cu^{I},[8] Zn^{II},[9] and Ni^{II}.[9,10] Their structures are depicted in Figure 1. They contain the common feature of a Cys-Gly-Cys sequence supporting a cis-planar $Ni^{II}-S_2N_2$

* To whom correspondence should be addressed. E-mail: holm@chemistry.harvard.edu.

(1) Holm, R. H. *Pure Appl. Chem.* **1995**, *67*, 217−224.
(2) Lee, S. C.; Holm, R. H. *Chem. Rev.* **2004**, *104*, 1135−1157.
(3) Ragsdale, S. W.; Kumar, M. *Chem. Rev.* **1996**, *96*, 2515−2539.
(4) Grahame, D. A. *Trends Biochem. Sci.* **2003**, *28*, 221−224.
(5) Abbreviations are given in Chart 1.
(6) Drennan, C. L.; Heo, J.; Sintchak, M. D.; Schreiter, E.; Ludden, P. W. *Proc. Natl. Acad. Sci. U.S.A.* **2001**, *98*, 11973−11978.
(7) (a) Dobbek, H.; Svetlitchnyi, V.; Gremer, L.; Huber, R.; Meyer, O. *Science* **2001**, *293*, 1281−1285. (b) Dobbek, H.; Svetlitchnyi, V.; Liss, J.; Meyer, O. *J. Am. Chem. Soc.* **2004**, *126*, 5382−5387.
(8) Doukov, T. I.; Iverson, T. M.; Seravalli, J.; Ragsdale, S. W.; Drennan, C. L. *Science* **2002**, *298*, 567−572.
(9) Darnault, C.; Volbeda, A.; Kim, E. J.; Legrand, P.; Vernède, X.; Lindahl, P. A.; Fontecilla-Camps, J. C. *Nat. Struct. Biol.* **2003**, *10*, 271−279.

10.1021/ic040055s CCC: $27.50
Published on Web 08/21/2004

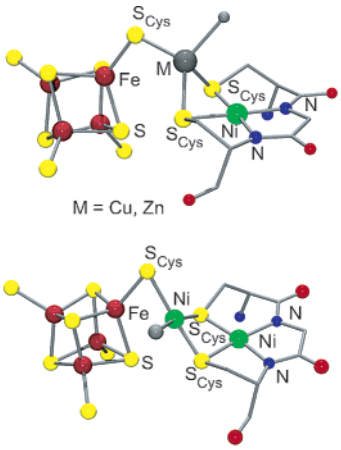

Figure 1. Structures of the $[Fe_4S_4]-(\mu_2\text{-}S_{Cys})-M-(\mu_2\text{-}S_{Cys})_2-Ni$ bridged assemblies in *Moorella thermoacetica* (f. *Clostridium thermoaceticum*) CODH/acetyl-CoA synthase: M = Cu^I, Zn^{II}, Ni^{II}. The terminal Ni^{II} atom is bound by a deprotonated Cys-Gly-Cys sequence; one ligand at the M site is unidentified.

coordination unit distal to the cluster, a nonplanar doubly bridged $Ni(\mu_2\text{-}S_{Cys})_2M$ rhomb, a proximal $M(\mu_2\text{-}S_{Cys})_3L$ unit with an unidentified nonprotein ligand L, and a singly bridged $[Fe_4S_4]-(\mu_2\text{-}S_{Cys})-M$ interaction. The stereochemistry at the proximal metal site is distorted tetrahedral with M = Cu^I and Zn^{II} and planar with M = Ni^{II} . Copper XAS data are consistent with the X-ray structure.[11] Further, the Ni XAS results for acetyl-CoA decarbonylase/synthase from *Methanosarcina thermophilia* are also compatible with the X-ray structure except that the bridging nickel atom is proposed to have an approximately tetrahedral stereochemistry.[12] Nickel L-edge XAS and MCD spectra of the as-isolated *M. thermophilia* enzyme indicate one low-spin site and one high-spin site,[13] which presumably are $Ni^{II}-S_2N_2$ and $Ni^{II}(\mu_2\text{-}S_{Cys})_3L$, respectively.

Three steps are essential to the construction of an A-cluster analogue: (i) creation of a planar $Ni^{II}-S_2N_2$ unit with physiologically credible coordination; (ii) addition of a bridging M atom to produce a doubly bridged $Ni(\mu_2\text{-}SR)_2M$ rhomb; (iii) construction of a $[Fe_4S_4]-(\mu_2\text{-}SR)-M$ bridge to a preformed cluster with the desired stereochemistry at atom M. An analogue of sufficient fidelity to a native assembly would then be subject to detailed investigations of structure, electronic features, and reactivity. Previous activities have focused on steps i and ii, with perhaps the most noteworthy results being the preparation of $Ni^{II}(\mu_2\text{-}SR)_2M$ rhombs with M = Cu^I and Ni^{II} that utilize cis-planar $Ni-S_2N_2$ components.[14−18] Step iii is the most problematic. One method has afforded the cluster $[\{(L_O-S_2N_2)Ni\}\text{-}Fe_4S_4I_3]^{1-}$ and related species in which, however, a $Ni^{II}-S_2N_2$ complex is doubly bridged through thiolate to an $[Fe_4S_4]^{2+}$ cluster.[19,20] In a more complicated approach, a *de novo* designed peptide has been employed as a scaffold to support a single cysteinate bridge between the cluster and an $Ni^{II}(S_{Cys})(N_{His})_2$ unit.[21,22]

Deliberate formation of bridged rhombs of the type $Ni^{II}\text{-}(\mu_2-SR)_2M$ can be traced back to the work of Jicha and Busch.[23] Thiolate bridges abound in contemporary Ni^{II} chemistry, especially homometallic bridges.[24,25] In seeking to create analogues of the A-cluster, we have investigated steps i and ii. In the process, a physiologically realistic complex has been prepared in step i. There having been no comparable examination heretofore, we have carried out an extensive investigation of thiolate bridging reactions of selected cis-planar $Ni^{II}-S_2N_2$ systems with, primarily, Cu^I and Ni^{II}, in relation to step ii. Since this work was initiated, convincing evidence has emerged that nickel is the native metal in the proximal site.[9,26−28] In a subsequent account, we will describe reactions directed at thiolate bridge formation to an $[Fe_4S_4]^{2+}$ cluster, a matter pertinent to the realization of step iii. Elsewhere, we report initial synthetic efforts directed toward the C-cluster of CODH.[29]

Experimental Section

Preparation of Compounds. All operations were conducted under a pure dinitrogen atmosphere using standard Schlenk line techniques or in an inert atmosphere box. Abbreviations are given in Chart 1. The compounds $(Et_4N)_2[Ni(L_H\text{-}S_2N_2)]$,[30] $[Ni(L_R\text{-}S_2N_2)]$,[31] $[(PPh_3)_3CuCl]$,[32] $[(PPh_3)_2Cu(SC\{O\}Ph)]$,[33] $[(PPh_3)_3AgCN]$,[32] $[Cu(CH_3\text{-}$

(10) Svetlitchnyi, V.; Dobbek, H.; Meyer-Klaucke, W.; Meins, T.; Thiele, B.; Römer, P.; Huber, R.; Meyer, O. *Proc. Natl. Acad. Sci. U.S.A.* **2004**, *101*, 446−451.
(11) Seravalli, J.; Gu, W.; Tam, A.; Strauss, E.; Begley, T. P.; Cramer, S. P.; Ragsdale, S. W. *Proc. Natl. Acad. Sci. U.S.A.* **2003**, *100*, 3689−3694.
(12) Gu, W.; Gencic, S.; Cramer, S. P.; Grahame, D. A. *J. Am. Chem. Soc.* **2003**, *125*, 15343−15351.
(13) Funk, T.; Gu, W.; Friedrich, S.; Wang, H.; Gencic, S.; Grahame, D. A.; Cramer, S. P. *J. Am. Chem. Soc.* **2004**, *126*, 88−95.
(14) Krishnan, R.; Voo, J. K.; Riordan, C. G.; Zahkarov, L.; Rheingold, A. L. *J. Am. Chem. Soc.* **2003**, *125*, 4422−4423.
(15) Linck, R. C.; Spahn, C. W.; Rauchfuss, T. B.; Wilson, S. R. *J. Am. Chem. Soc.* **2003**, *125*, 8700−8701.
(16) Golden, M. L.; Rampersad, M. V.; Reibenspies, J. H.; Darensbourg, M. Y. *Chem. Commun.* **2003**, 1824−1826.
(17) Wang, Q.; Blake, A. J.; Davies, E. S.; McInnes, E. J. L.; Wilson, C.; Schröder, M. *Chem. Commun.* **2003**, 3012−3013.
(18) Krishnan, R.; Riordan, C. G. *J. Am. Chem. Soc.* **2004**, *126*, 4484−4485.
(19) Osterloh, F.; Saak, W.; Haase, D.; Pohl, S. *Chem. Commun.* **1996**, 777−778.
(20) Osterloh, F.; Saak, W.; Pohl, S. *J. Am. Chem. Soc.* **1997**, *119*, 5648−5656.
(21) Laplaza, C. E.; Holm, R. H. *J. Am. Chem. Soc.* **2001**, *123*, 10255−10264.
(22) Musgrave, K. B.; Laplaza, C. E.; Holm, R. H.; Hedman, B.; Hodgson, K. O. *J. Am. Chem. Soc.* **2002**, *124*, 3083−3092.
(23) Jicha, D. C.; Busch, D. H. *Inorg. Chem.* **1962**, *1*, 872−877.
(24) Tremel, W.; Kriege, M.; Krebs, B.; Henkel, G. *Inorg. Chem.* **1988**, *27*, 3886−3895.
(25) Meyer, F.; Kozlowski, H. Nickel. In *Transition Metal Groups 9−12*; Fenton, D. E., Ed.; Elsevier, Ltd.: Oxford, 2004; pp 247−554.
(26) Bramlett, M. R.; Tan, X.; Lindahl, P. A. *J. Am. Chem. Soc.* **2003**, *124*, 9316−9317.
(27) Schenker, R. P.; Brunold, T. C. *J. Am. Chem. Soc.* **2003**, *125*, 13962−13963.
(28) Seravalli, J.; Xiao, Y.; Gu, W.; Cramer, S. P.; Antholine, W. E.; Krymov, V.; Gerfern, G. J.; Ragsdale, S. W. *Biochemistry* **2004**, *43*, 3944−3955.
(29) Panda, R.; Zhang, Y.; McLauchlan, C. C.; Venkateswara Rao, P.; Tiago de Oliveira, F. A.; Münck, E.; Holm, R. H. *J. Am. Chem. Soc.* **2004**, *126*, 6448−6459.
(30) Krüger, H.-J.; Peng, G.; Holm, R. H. *Inorg. Chem.* **1991**, *30*, 734−743.
(31) Fox, S.; Stibrany, R. T.; Potenza, J. A.; Knapp, S.; Schugar, H. J. *Inorg. Chem.* **2000**, *39*, 4950−4961.
(32) Reichle, W. *Inorg. Chim. Acta* **1971**, *5*, 325−332.
(33) Deivaraj, T. C.; Lai, G. X.; Vittal, J. J. *Inorg. Chem.* **2000**, *39*, 1028−1034.

Chart 1. Designation of Complexes, Ligands, and Abbreviations

$[Ni(L_H\text{-}S_2N_2)]^{2-}$	**1**[30]
$[\{Ni(L_H\text{-}S_2N_2)\}_2Ag]^{3-}$	**2**
$[\{Ni(L_H\text{-}S_2N_2)\}_2Cu_2]^{2-}$	**3**
$[\{Ni(L_H\text{-}S_2N_2)\}_2Hg_2Cl_3]^{3-}$	**4**
$[Ni(L_R\text{-}S_2N_2)]$	**5**[31]
$[\{Ni(L_R\text{-}S_2N_2)\}Zn(OTf)(H_2O)]_2^{2+}$	**6**
$[\{Ni(L_R\text{-}S_2N_2)\}ZnCl_2]_2$	**7**
$[\{Ni(L_R\text{-}S_2N_2)\}ZnCl_2(DMF)]$	**8**
$[\{Ni(L_R\text{-}S_2N_2)\}HgCl_2]_4$	**9**
$[\{Ni(L_R\text{-}S_2N_2)\}_3Cu_2]^{2+}$	**10**
$[\{Ni(L_R\text{-}S_2N_2)\}\{Cu(OPh)(PPh_3)\}_2]$	**11**
$[\{Ni(L_R\text{-}S_2N_2)\}Cu(SC\{O\}Ph)(PPh_3)]$	**12**
$[\{Ni(L_R\text{-}S_2N_2)\}CuCN(PPh_3)]$	**13**
$[\{Ni(L_R\text{-}S_2N_2)\}CuCl(PPh_3)]$	**14**
$[\{Ni(L_R\text{-}S_2N_2)\}Cu(S\text{-}p\text{-}tol)(PPh_3)]$	**15**
$[\{Ni(L_R\text{-}S_2N_2)\}Ni(MeCN)\{Ni(L_R\text{-}S_2N_2)\}]^{2+}$	**16**
$[\{Ni(L_R\text{-}S_2N_2)\}Ni(PMe_3)_2(MeCN)]^{2+}$	**17**
$[\{Ni(L_R\text{-}S_2N_2)\}NiCl(PPh_3)]^{1+}$	**18**
$[\{Ni(L_R\text{-}S_2N_2)\}Ni(S\text{-}p\text{-}tol)]_2^{2+}$	**19**
$[\{Ni(L_R\text{-}S_2N_2)\}Ni(depe)]^{2+}$	**20**
$[\{Ni(L_R\text{-}S_2N_2)\}Ni(dppe)]^{2+}$	**21**
$H_4(L\text{-}655)$*	**22g**
$[\{Ni(L\text{-}655)\}_2Ni]^{2-}$	**23**
$[Ni(L\text{-}655)]^{2-}$	**24**
$[\{Ni(L\text{-}655)\}Ni(depe)]$	**25**
$[\{Ni(L\text{-}655)\}Ni(dppe)]$	**26**
$[\{Ni(L\text{-}655)\}_2Cu]^{2-}$	**27**

*Four replaceable protons in the formation of Ni^{II} complexes.

Abbreviations: ACS, acetylcoenzyme A synthase; CoA, coenzyme A; CODH, carbon monoxide dehydrogenase; depe, 1,2-bis(diethylphosphino)ethane; dppe, 1,2-bis(diphenylphosphino)ethane; $L_H\text{-}S_2N_2$, *N,N′*-ethylenebis(2-mercaptoisobutyramide)(4-) (ligand prepared at Harvard (H)); $L_O\text{-}S_2N_2$, *N,N′*-diethyl-3,7-diazanonane-1,9-dithiolate(2-) (ligand prepared by Osterloh *et al.* (O)); $L_R\text{-}S_2N_2$, *trans-rac-N,N*-bis(2-mercapto-2-methylprop-1-yl)-1,2-cyclohexanediamine(2-) (ligand prepared at Rutgers (R)); L-655, *N*-(2-mercaptopropyl)-*N′*-(2′-mercaptoethyl)glycinamide(4-); nbt, bicyclo[2.2.1]hepta-*exo-cis*-2,3-dithiolate(2-); SCE, standard calomel electrode; Su, succinimido; tip, 2,4,6-triisopropylphenyl; tol, tolyl; XAS, X-ray absorption spectra.

$CN)_4](PF_6)$,[34] $[(PPh_3)_3Cu(OPh)]$,[35] $[(PPh_3)_3CuCN]$,[32] $[Ni(depe)Cl_2]$,[36] and bicyclo[2.2.1]hepta-*exo-cis*-2,3-dithiol[37] were synthesized by literature procedures. All solvents were distilled prior to use. Methanol, ethanol, and hexanes were distilled from sodium/potassium alloy while acetonitrile, dichloromethane, and ether were passed through an Innovative Technology solvent purification system. Volume reductions were performed in situ; filtrations of reaction mixtures were made through Celite. For compound isolation, ether was introduced by vapor diffusion unless noted otherwise. Isolated products were washed with ether and dried. All complexes were identified by positive-ion electrospray mass spectrometry (percentages refer to peak intensity relative to the most intense fragment peak) and by crystal structure determinations (with two exceptions).

Bridged $Ni^{II}S_2N_2-Ni^{II}/Cu^{I}/Zn^{II}/Ag^{I}/Hg^{II}$ Complexes. (A) Derived from $[Ni(L_H\text{-}S_2N_2)]^{2-}$ (1). $(Et_4N)_3[\{Ni(L_H\text{-}S_2N_2)\}_2Ag]$ ($(Et_4N)_3$[2]). To a red solution of $(Et_4N)_2[Ni(L_H\text{-}S_2N_2)]$ (0.062 g, 0.10 mmol) in 5 mL of acetonitrile was added a suspension of $[AgCN(PPh_3)_3]$ (0.092 g, 0.10 mmol) in 2 mL of acetonitrile. Within a few minutes, the white suspension completely disappeared, and the resulting orange-red solution was stirred for 4 h. The reaction mixture was filtered, and ether was introduced into the filtrate. The product was obtained as 0.045 g (79%) of orange-red crystals. Mass spectrum: *m/z* 860 ($\{M + H\}^+$, 10%).

$(Et_4N)_2[\{Ni(L_H\text{-}S_2N_2)\}_2Cu_2]$ ($(Et_4N)_2$[3]). Method A. To a red solution of $(Et_4N)_2[Ni(L_H\text{-}S_2N_2)]$ (0.308 g, 0.500 mmol) in 15 mL of acetonitrile was added a clear, colorless solution of $[CuCl(PPh_3)_3]$ (0.443 g, 0.500 mmol) in 8 mL of THF. The orange-red reaction mixture was stirred for 3 h and was filtered. Ether was introduced into the filtrate, causing separation of orange-red crystals. These were washed with ether and dried to give 0.198 g (77%) of product.

Method B. To a solution of $(Et_4N)_2[Ni(L_H\text{-}S_2N_2)]$ (0.047 g, 0.076 mmol) in 3 mL of acetonitrile was added a suspension of $[(PPh_3)_2Cu(SC\{O\}Ph)]$ (0.055 g, 0.076 mmol) in 1.5 mL of acetonitrile. Within a few minutes, the solid dissolved to give an orange-red solution, which was stirred for 4 h. The reaction mixture was filtered, and ether was added to filtrate, causing separation of a solid. The product was obtained as 0.028 g (72%) of orange-red crystals. Mass spectrum: *m/z* 767 ($\{M + H\}^+$, 50%).

$(Et_4N)_3[\{Ni(L_H\text{-}S_2N_2)\}_2Hg_2Cl_2(\mu_2\text{-}Cl)]$ ($(Et_4N)_3$[4]). To a red solution of $(Et_4N)_2[Ni(L_H\text{-}S_2N_2)]$ (0.075 g, 0.122 mmol) in 5 mL of acetonitrile was added a solution of $HgCl_2$ (0.033 g, 0.122 mmol) in 1 mL of acetonitrile. The orange-red solution was stirred for 4 h, the reaction mixture was filtered, and ether was introduced into the filtrate. The product was obtained as 0.078 g (83%) of orange-red crystals. Mass spectrum: *m/z* 1112 ($\{M - Cl\}^+$, 10%).

(B) Derived from $[Ni(L_R\text{-}S_2N_2)]$ (5). $[\{Ni(L_R\text{-}S_2N_2)\}Zn(OTf)(H_2O)]_2(OTf)_2$ ([6](OTf)$_2$). To a suspension of $[Ni(L_R\text{-}S_2N_2)]$ (0.050 g, 0.144 mmol) in 5 mL of acetonitrile was added a suspension of $Zn(OTf)_2$ (0.052 g, 0.144 mmol) in 2 mL of acetonitrile. Within a few minutes, the reaction mixture became a dark red solution, which was stirred for 3 h. The mixture was filtered through Celite, and the filtrate was concentrated to dryness. The pink solid was dissolved in THF and filtered. Diffusion of pentane into the filtrate gave 0.079 g (75%) of a pink microcrystalline solid. Mass spectrum: *m/z* 379 ($\{(M - Zn(OTf)_4)/2\}^{2+}$, 50%).

$[\{Ni(L_R\text{-}S_2N_2)\}ZnCl_2]_2$ (7). To a suspension of $[Ni(L_R\text{-}S_2N_2)]$ (0.208 g, 0.60 mmol) in 25 mL of acetonitrile was added dropwise a solution of $ZnCl_2$ (0.082 g, 0.60 mmol) in 10 mL of acetonitrile. Within a few minutes, the reaction mixture turned to a dark red solution. The mixture was stirred for 3 h and filtered. Ether was layered on the filtrate, causing the product to separate as 0.190 g (65%) of a purple crystalline solid. Mass spectrum: *m/z* 793 ($\{M - ZnCl_3\}^+$, 25%).

$[\{Ni(L_R\text{-}S_2N_2)\}HgCl_2]_4$ (9). To a suspension of $[Ni(L_R\text{-}S_2N_2)]$ (0.050 g, 0.144 mmol) in 5 mL of acetonitrile was added dropwise a solution of $HgCl_2$ (0.039 g, 0.14 mmol) in 3 mL of acetonitrile. The reaction mixture turned to a clear red solution, and within a few minutes a pink solid separated. The reaction mixture was stirred for 3 h. The solid that separated was washed thoroughly with ether and recrystallized from dichloromethane/ether to afford the product as 0.066 g (74%) of pink solid. Mass spectrum: *m/z* 929 ($\{M - HgCl_3\}^+$, 100%).

$[\{Ni(L_R\text{-}S_2N_2)\}_3Cu_2](PF_6)_2$ ([10](PF$_6$)$_2$). To a suspension of $[Ni(L_R\text{-}S_2N_2)]$ (0.058 g, 0.167 mmol) in 5 mL of acetonitrile was added dropwise a solution of $[Cu(MeCN)_4](PF_6)$ (0.062 g, 0.167 mmol) in 4 mL of acetonitrile. The deep red solution was stirred for 3 h and filtered. Ether diffusion into the filtrate gave the product as 0.065 g (53%) of red crystals. Mass spectrum: *m/z* 583 ($\{M/2\}^{2+}$, 100%).

$[\{Ni(L_R\text{-}S_2N_2)\}\{Cu(OPh)(PPh_3)\}_2]$ (11). To a suspension of $[Ni(L_R\text{-}S_2N_2)]$ (0.050 g, 0.144 mmol) in 5 mL of toluene was added a solution of $[(PPh_3)_3Cu(OPh)]$ (0.136 g, 0.144 mmol) in 3 mL of toluene. The initial suspension turned to a dark red solution, and the reaction mixture was stirred for 5 h. It was filtered, and hexane was vapor-diffused into the filtrate. The product was obtained as 0.076 g (45%) of dark red crystals. Mass spectrum: *m/z* 671 ($\{M - Cu(OPh)_2(PPh_3) + H\}^+$, 25%).

$[\{Ni(L_R\text{-}S_2N_2)\}Cu(SC\{O\}Ph)(PPh_3)]$ (12). To a suspension of $[Ni(L_R\text{-}S_2N_2)]$ (0.050 g, 0.144 mmol) in 6 mL of dichloromethane

(34) Kubas, G. J. *Inorg. Synth.* **1979**, *19*, 90−92.
(35) Osakada, K.; Takizawa, T.; Tanaka, M.; Yamamoto, T. *J. Organomet. Chem.* **1994**, *473*, 359−369.
(36) Alyea, E. C.; Meek, D. W. *Inorg. Chem.* **1972**, *11*, 1029−1033.
(37) Shields, T. C.; Kurtz, A. N. *J. Am. Chem. Soc.* **1969**, *91*, 5415−5416.

was added dropwise a yellow solution of $[(PPh_3)_2Cu(SC\{O\}Ph)]$ (0.104 g, 0.144 mmol) in 2 mL of dichloromethane. The reaction mixture turned to a red solution and was stirred for 3 h. It was filtered, and ether was layered onto the filtrate. The product was obtained as 0.087 g (74%) of brown crystals. Mass spectrum: *m*/*z* 671 ($\{M - SCOPh\}^+$, 90%).

[$\{Ni(L_R\text{-}S_2N_2)\}CuCN(PPh_3)$] (13). To a suspension of [$Ni(L_R\text{-}S_2N_2)$] (0.050 g, 0.144 mmol) in 10 mL of dichloromethane was added dropwise a solution of [$CuCN(PPh_3)_3$] (0.126 g, 0.144 mmol) in 5 mL of dichloromethane. The reaction mixture turned to a red solution and was stirred for 3 h. It was filtered through Celite, and ether was layered on top of the filtrate. The product was isolated as 0.080 g (81%) of a purple crystalline solid. Mass spectrum: *m*/*z* 671 ($\{M - CN\}^+$, 70%).

[$\{Ni(L_R\text{-}S_2N_2)\}CuCl(PPh_3)$] (14). To a suspension of [$Ni(L_R\text{-}S_2N_2)$] (0.416 g, 1.20 mmol) in 25 mL of dichloromethane was added dropwise a solution of [$CuCl(PPh_3)_3$] (1.06 g, 1.20 mmol) in 15 mL of dichloromethane. Within a few minutes, the reaction mixture turned to a red solution that was stirred for 3 h and filtered. Ether was layered onto the filtrate, causing separation of the product as 0.712 g (84%) of purple needlelike crystals. Mass spectrum: *m*/*z* 671 ($\{M - Cl\}^+$, 100%).

[$\{Ni(L_R\text{-}S_2N_2)\}Cu(S\text{-}p\text{-}tol)(PPh_3)$] (15). To a suspension of [$\{Ni(L_R\text{-}S_2N_2)\}CuCl(PPh_3)$] (0.050 g, 0.070 mmol) in 5 mL of acetonitrile was added a suspension of Na(S-*p*-tol) (0.011 g, 0.078 mmol) in 1 mL of acetonitrile. The mixture was stirred for 12 h and filtered. The orange filtrate was concentrated to dryness, resulting in 0.040 g (71%) pink needle-shaped crystals. Mass spectrum: *m*/*z* 671 ($\{M - (S\text{-}p\text{-}tol)\}^+$, 50%).

[$\{Ni(L_R\text{-}S_2N_2)\}Ni(MeCN)\{Ni(L_R\text{-}S_2N_2)\}$](OTf)$_2$ ([16](OTf)$_2$). To a suspension of [$Ni(L_R\text{-}S_2N_2)$] (0.050 g, 0.144 mmol) in 5 mL of acetonitrile was added dropwise a pale bluish solution of $Ni(OTf)_2$ (0.051 g, 0.144 mmol) in 5 mL of acetonitrile. The reaction mixture turned to a clear dark brown solution and was stirred for 3 h. It was then filtered, and ether was added to the filtrate. The product was obtained as 0.055 g (35%) of brown crystals. Mass spectrum: *m*/*z* 693 ($\{M - Ni(OTf)_2 + H^+\}^+$, 100%).

[$\{Ni(L_R\text{-}S_2N_2)\}Ni(PMe_3)_2(MeCN)$](PF$_6$)$_2$ ([17](PF$_6$)$_2$). To a suspension of [$Ni(L_R\text{-}S_2N_2)$] (0.035 g, 0.10 mmol) in 5 mL of acetonitrile was added dropwise an orange-red solution of [$Ni(PMe_3)_2Cl_2$] (0.028 g, 0.10 mmol) in 5 mL of acetonitrile. To the resulting red suspension was added a suspension of $NaPF_6$ (0.034 g, 0.2 mmol) in 2 mL of acetonitrile, and the deep red solution was stirred for 2 h. The mixture was filtered through Celite, the filtrate was concentrated to dryness, and the residue was extracted with acetonitrile. Diffusion of ether into the extract gave 0.055 g (62%) of red crystals. Mass spectrum: *m*/*z* 346 ($\{M - Ni(PMe_3)_2(MeCN)\}^+$, 100%).

[$\{Ni(L_R\text{-}S_2N_2)\}NiCl(PPh_3)$](PF$_6$) ([18](PF$_6$)). To a suspension of [$Ni(L_R\text{-}S_2N_2)$] (0.200 g, 0.576 mmol) in 30 mL of THF was added a suspension of [$Ni(PPh_3)_2Cl_2$] (0.377 g, 0.576 mmol) in 5 mL of THF. To the resulting red suspension was added a suspension of $NaPF_6$ (0.193 g, 1.15 mmol) in 5 mL of THF, and the deep red solution was stirred for 6 h. The mixture was filtered through Celite, and the filtrate was concentrated to dryness to give 0.366 g (75%) of a green-black solid. Mass spectrum: *m*/*z* 671 ($\{M - Cl\}^+$, 10%), 693 ($\{M - Cl + Na\}^+$, 25%).

[$\{Ni(L_R\text{-}S_2N_2)\}Ni(S\text{-}p\text{-}tol)$]$_2$(PF$_6$)$_2$ ([19](PF$_6$)$_2$). To a solution of [$\{Ni(L_R\text{-}S_2N_2)\}NiCl(PPh_3)$] (0.058 g, 0.068 mmol) in 5 mL of acetonitrile was added a suspension of Na(S-*p*-tol) (0.010 g, 0.068 mmol) in 5 mL of acetonitrile. Within a few minutes, the brown mixture turned to a dark red solution, which was stirred for 6 h and filtered. The dark red filtrate was concentrated to dryness, and the residue was extracted with acetonitrile**.** Vapor diffusion of ether into the filtrate gave the product as 0.028 g (61%) of dark-brown platelike crystals. Mass spectrum: *m*/*z* 347 ($\{M/2\text{-}Ni(S\text{-}p\text{-}tol)(PF_6)\}^{2+}$, 100%), 695 ($\{M/2 - PF_6 + Na\}^{2+}$, 20%).

[$\{Ni(L_R\text{-}S_2N_2)\}Ni(depe)$](PF$_6$)$_2$ ([20](PF$_6$)$_2$). To a suspension of [$Ni(L_R\text{-}S_2N_2)$] (0.035 g, 0.10 mmol) in 5 mL of acetonitrile was added dropwise an orange-yellow solution of [$Ni(depe)Cl_2$] (0.042 g, 0.10 mmol) in 5 mL of acetonitrile. To the resulting orange suspension was added a suspension of $NaPF_6$ (0.034 g, 0.2 mmol) in 2 mL of acetonitrile, and the dark red solution was stirred for 2 h. The mixture was filtered through Celite, and the filtrate was concentrated to dryness to give 0.052 g (58%) of a red glassy solid. Mass spectrum: *m*/*z* 347 ($\{M\text{-}Ni(depe)(PF_6)_2\}^+$, 100%), 650 ($\{M + K\}^+$, 40%).

[$\{Ni(L_R\text{-}S_2N_2)\}Ni(dppe)$](PF$_6$)$_2$ ([21](PF$_6$)$_2$). To a suspension of [$Ni(L_R\text{-}S_2N_2)$] (0.035 g, 0.10 mmol) in 5 mL of THF was added dropwise an orange-red suspension of [$Ni(dppe)Cl_2$] (0.053 g, 0.10 mmol) in 5 mL of THF. To the resulting orange suspension was added a suspension of $NaPF_6$ (0.034 g, 0.2 mmol) in 2 mL of acetonitrile, and the dark red solution was stirred for 3 h. The mixture was filtered through Celite, and the filtrate was concentrated to dryness to give 0.072 g (66%) of a red solid. Mass spectrum: *m*/*z* 427 ($\{M + 2Na^+/2\}^{2+}$, 100%).

(C) Diamidodithiol H$_4$(L-655) and Its Ni^{II} Complexes. The overall procedure for the ligand synthesis is related to that reported for the preparation of *N*-(2-mercaptoacetyl)-*N*′-(2-mercaptoethyl)-glycinamide.[38]

3-Triphenylmethylthiopropionic acid (**22a**)**.** To a suspension of triphenylmethanol (30.0 g, 0.115 mol) in 40 mL of glacial acetic acid was added 3-mercaptopropionic acid (10 mL, 0.115 mol). The mixture was heated to ~75 °C after which a solution of boron trifluoride etherate (16 mL, 0.125 mmol) was added dropwise, and the thick yellow solution was stirred for 2 h at room temperature. The reaction mixture was poured into 300 mL of water to yield a voluminous white precipitate. This material was washed copiously with water (150 mL) and ether (100 mL) and dried in vacuo. The ether washings gave a further crop. The compound was recrystallized from petroleum ether/hexanes to give 38 g (95%). ^{1}H NMR (d_6-DMSO): δ 2.17 (t, 2H, CH_2), 2.27 (t, 2H, CH_2), 7.33 (m, 15H, aryl), 12.2 (s, 1H, CO_2H). Mass spectrum: *m*/*z* 157 ($\{(M - CO_2 - 2H)/2\}^{2+}$, 100%), 243 ($\{CPh_3\}^+$, 10%). This compound has been prepared previously by a somewhat different method.[39]

Succinimido-3-(triphenylmethylthio)propionate (**22b**). To an ice-cold solution of **22a** (34.9 g, 0.10 mol) and *N*-hydroxysuccinimide (11.5 g, 0.10 mol) in dimethoxyethane (250 mL) was added a cooled solution of dicyclohexylcarbodiimide (22.7 g, 0.11 mol) in dimethoxyethane (50 mL). The temperature was maintained below −5 °C throughout the addition. The white suspension was stirred at 4 °C overnight and filtered to give a colorless filtrate. The white precipitate was extensively washed with dichloromethane (200 mL), and the filtrate and washings were combined and evaporated in vacuo. The product was obtained as 28 g (63%). ^{1}H NMR (d_6-DMSO): δ 2.18 (t, 2H, CH_2), 2.30 (t, 2H, CH_2), 2.80 (t, 4H, CH_2Su), 7.35 (m, 15H, aryl). Mass spectrum: *m*/*z* 303 ($\{Ph_3CSHEt\}^+$, 100%), 449 ($\{Ph_3CSCH_2CH_2CO_2Su + H\}^+$, 25%).

[3-(Triphenylmethylthio)propionyl]glycine (**22c**)**.** To an ice-cold solution of the activated ester compound **22b** (31.2 g, 0.070 mol) in dimethoxyethane (300 mL) and DMF (150 mL) was added a solution of glycine (5.25 g, 0.070 mol) and $NaHCO_3$ (11.8 g,

(38) Brenner, D.; Davison, A.; Lister-James, J.; Jones, A. G. *Inorg. Chem.* **1984**, *23*, 3793−3797.
(39) Bray, A. M.; Kelly, D. P.; Mack, P. O. L.; Martin, R. F.; Wakelin, L. P. G. *Austr. J. Chem.* **1990**, *43*, 629−634.

0.140 mol) in water (150 mL). The reaction mixture was stirred for 1 h at −10 °C and concentrated in vacuo to remove the dimethoxyethane. The pale yellow solution was diluted with water (150 mL) and treated with 50% aqueous citric acid (60 mL). A voluminous solid was collected and washed with petroleum ether to give 26 g of product (92%). ^{1}H NMR (d_6-DMSO): δ 2.20 (t, 2H, CH_2), 2.40 (t, 2H, CH_2), 3.60 (d, 2H, CH_2 Gly), 7.33 (m, 15H, aryl), 13.2 (br, 1H, CO_2H). Mass spectrum: *m*/*z* 303 ({Ph_3CSHEt}$^+$, 100%).

[3-(Triphenylmethylthio)propionyl]glycine, *N*-hydroxysuccinimide ester (22d). To a cooled solution of **22c** (20.0 g, 0.049 mol) and *N*-hydroxysuccinimide (5.63 g, 0.049 mol) in 200 mL of dimethoxyethane was added dropwise a solution of dicyclohexylcarbodiimide (12.7 g, 0.56 mol) in 40 mL of dimethoxyethane such that the temperature remained below 0 °C. The yellowish suspension was stirred overnight at 4 °C. It was filtered to give a colorless filtrate and a white precipitate that was thoroughly washed with dichloromethane (150 mL). The filtrate and washings were combined, and solvent was removed in vacuo to give a yellowish solid, which was washed with ethyl acetate and ether and dried in vacuo. The product was obtained as 16 g of solid (65%). ^{1}H NMR (d_6-DMSO): δ 2.20 (m, 4H, CH_2), 2.70 (m, 4H, CH_2 Su), 4.20 (d, 2H, CH_2 Gly), 7.30 (m, 15H, aryl), 8.7 (t, 1H, NH). Mass spectrum: *m*/*z* 303 ({Ph_3CSHEt}$^+$, 100%), 502 ({$Ph_3CSCH_2CH_2CO_2Su + H$}$^+$, 25%).

2-(Triphenylmethylthio)ethylamine (22e). A mixture of 2-mercaptoethylamine hydrochloride (11.5 g, 0.10 mol) and triphenylmethanol (26.3 g, 0.10 mol) in trifluoroacetic acid (100 mL) was stirred at room temperature for 30 min and evaporated to a dark brown oil. Addition of ether (500 mL) resulted in immediate discharge of color and formation of a white precipitate that was filtered off, washed with ether, and dried. The ether washings gave a further crop, with a combined yield of 29.5 g (67%). The trifluoroacetate salt (14.0 g, 32.0 mmol) obtained in this manner was partitioned between 1 M aqueous NaOH and ether. Evaporation of the ether phase and recrystallization from ether/hexanes gave the product as 9.0 g (87%) of a white crystalline compound. ^{1}H NMR (d_6-DMSO): δ 1.05 (s, 2H, NH_2), 2.45 (m, 4H, CH_2), 7.23 (m, 15H, aryl). Mass spectrum: *m*/*z* 320 ({$Ph_3CS(CH_2)_2NH_3$}$^+$, 30%), 243 ({CPh_3}$^+$, 100%).

***N*-[3-(Triphenylmethylthio)propionyl]-*N*′-[2-(triphenylmethylthio)ethyl]glycinamide (22f).** A solution of ester **22d** (3.65 g, 7.3 mmol) and amine **22e** (2.33 g, 7.3 mmol) were combined in dichloromethane (100 mL); the yellowish solution was stirred at 0 °C for 3 h and stored at −20 °C overnight. The white precipitate was filtered off, washed copiously with dichloromethane (100 mL), and dried. The filtrate, washed with 5% $NaHCO_3$ solution (3 × 50 mL), dried overnight over Na_2SO_4, evaporated in vacuo, and recrystallized from dichloromethane gave a further batch for a total yield of 5.0 g (97%). ^{1}H NMR (d_6-DMSO): δ 2.10−2.20 (m, 6H, CH_2), 2.96 (q, 2H, CH_2), 3.56 (d, 2H, CH_2 Gly), 7.33 (m, 10H, aryl), 7.90 (t, 1H, NH), 8.10 (t, 1H, NH). Mass spectrum: *m*/*z* 708 ({M + H}$^+$, 70%), 243 ({CPh_3}$^+$, 50%).

[*N*-(2-Mercaptopropyl)-*N*′-(2′-mercaptoethyl)]glycinamide (22g). To a solution of **22f** (3.80 g, 5.38 mmol) was added trifluoroacetic acid (20 mL); the mixture was cooled in an ice-bath at 0 °C. To it was added dropwise triethylsilane (2.0 mL, 12.5 mmol), causing the appearance of a white precipitate. The mixture was diluted with hexanes (35 mL) and water (35 mL), and the aqueous layer was separated and washed with hexanes (3 × 30 mL). The combined aqueous extract was filtered and evaporated in vacuo to yield a colorless oil. The oil was triturated with ether to yield an off-white solid that was collected, washed with ether, and dried in vacuo, giving the product as 0.86 g (72%). ^{1}H NMR ($CDCl_3$): δ 2.58 (t, 2H, CH_2), 2.68 (q, 2H, CH_2), 2.84 (q, 2H, CH_2), 3.47 (q, 2H, CH_2), 3.97 (d, 2H, CH_2-Gly), 6.58 (br, 1H, NH), 6.76 (br, 1H, NH). Mass spectrum: *m*/*z* 223.0574 ({M + H}$^+$, calcd 223.0575). Elemental analysis gave the atom ratio S/N = 0.994; percentages indicated an water/ether solvate. Anal. Calcd for $C_7H_{14}N_2O_2S_2 \cdot {}^1/_2H_2O$ (example): C, 36.34; H, 6.54; N, 12.11; S, 27.72. Found: C, 37.04; H, 5.95; N, 11.84; S, 26.94.

$(Et_4N)_2$[{Ni(L-655)}$_2$Ni] ($(Et_4N)_2$[23]). To a solution of **22g** (1.30 g, 5.85 mmol) in 20 mL of methanol was added a solution of NaOMe (1.33 g, 24.6 mmol) in 30 mL of methanol. To the clear yellow solution was added a methanolic solution (5 mL) of Et_4NCl (1.94 g, 11.7 mmol), resulting in the appearance of a turbid yellow solution. This solution was stirred for 20 min, and to it was added dropwise a solution of $Ni(OAc)_2 \cdot 4H_2O$ (1.46 g, 5.85 mmol) in 60 mL of methanol. The initial pale yellow color of the solution changed to red and then to dark green as the addition was completed. This mixture was allowed to stir for 2 h, and solvent was removed in vacuo. The residue was extracted with acetonitrile. The extract was filtered and layered with ether to cause the precipitation of the product as 1.10 g (44%) of a green solid. ^{1}H NMR (DMSO-d_6, anion): δ 1.72−2.50 (m, 16), 3.42 (t, 4), Mass spectrum: *m*/*z* 615 ({M + H}$^+$, 75%), 308 ({(M + 2H$^+$)/2}$^{2+}$, 100%).

$(Et_4N)_2$[Ni(L-655)] ($(Et_4N)_2$[24]). To a solution of **22g** (0.244 g, 1.1 mmol) in 20 mL of methanol was added a solution of NaOMe (0.238, 4.40 mmol) in 5 mL of methanol. This mixture was added slowly to a green solution of $(Et_4N)_2$[{Ni(L-655)}$_2$Ni] (0.873 g, 1.00 mmol) in 75 mL of acetonitrile. The green color changed to red. The reaction mixture was stirred for 10 min, and a solution of Et_4NCl (0.729 g, 4.00 mmol) in acetonitrile (10 mL) was added, causing a precipitate of NaCl. The mixture was stirred for 30 min, and solvent was evaporated to dryness. The pale pink solid was extracted with acetonitrile and the extract was filtered. Ether was layered on top of the filtrate. The solid that separated was washed twice with ether and dried to give the product as 1.27 g (79%) of pink solid. ^{1}H NMR (CD_3CN, anion): δ 1.65 (t, 2H), 1.80 (t, 2H), 2.03 (t, 2H), 2.69 (t, 2H), 3.37 (s, 2H). Mass spectrum: *m*/*z* 538 ({M + H}$^+$, 100%).

[{Ni(L-655)}Ni(depe)] (25). To a solution of $(Et_4N)_2$[Ni(L-655)] (0.027 g, 0.05 mmol) in 4 mL of acetonitrile was added dropwise an orange-yellow solution of [Ni(depe)Cl_2] (0.021 g, 0.05 mmol) in 2 mL of acetonitrile. The resulting dark red solution was stirred for 1 h, the reaction mixture was filtered, and ether was introduced into the filtrate. The product was obtained as 0.025 g (62%) of red crystals. Mass spectrum: *m*/*z* 543 ({M + H}$^+$, 100%).

[{Ni(L-655)}Ni(dppe)] (26). To a solution of $(Et_4N)_2$[Ni(L-655)] (0.054 g, 0.10 mmol) in 10 mL of acetonitrile was added a suspension of [Ni(dppe)Cl_2] (0.053 g, 0.10 mmol) in 5 mL of acetonitrile. The dark brown reaction mixture was stirred for 10 h and filtered, and the filtrate was evaporated to dryness. The residue was washed with acetonitrile and ether and was dried. The solid was extracted with dichloromethane and filtered. Ether was introduced into the filtrate, causing separation of the product as 0.042 g (58%) of red-brown crystals.

$(Et_4N)_2$[{Ni(L-655)}$_2$Cu] ($(Et_4N)_2$[27]). To a solution of $(Et_4N)_2$[Ni(L-655)] (0.050 g, 0.093 mmol) in 10 mL of acetonitrile was added dropwise a solution of $Cu(OTf)_2$ (0.017 g, 0.046 mmol) in 5 mL of acetonitrile. The dark green solution was stirred for 10 h and filtered, and ether was layered onto the filtrate. The product was obtained as 0.034 g (85%) of green microcrystals. Mass spectrum: *m*/*z* 339 ({M − $(Et_4N)_2$[Ni(L-655)] + H}$^+$, 85%).

Table 1. Crystallographic Data for Compounds Containing Complexes **1**−**12**[a]

	$(Et_4N)_2$[**1**]·CH_3CN	$(Et_4N)_3$[**2**]	$(Et_4N)_2$[**3**]	$(Et_4N)_3$[**4**]·1.5CH_3CN·0.5H_2O	[**5**]·$Na(PF_6)$	[**6**]$(OTf)_2$·2Et_2O
formula	$C_{28}H_{59}N_5NiO_2S_2$	$C_{34}H_{80}AgN_7Ni_2O_4S_4$	$C_{36}H_{72}Cu_2N_6Ni_2O_4S_4$	$C_{47}H_{97.5}Cl_3Hg_{2-}N_{8.5}Ni_2O_{4.5}S_4$	$C_{14}H_{28}F_6N_2NaNiPS_2$	$C_{40}H_{80}F_{12}N_4Ni_2O_{16}S_8Zn_2$
cryst syst	orthorhombic	triclinic	triclinic	orthorhombic	orthorhombic	monoclinic
fw	620.63	1004.58	1025.74	1607.03	515.17	1605.72
space group	$P2_12_12_1$	$P\bar{1}$	$P\bar{1}$	$Pbc2_1$	$Cmc2_1$	$C2/c$
a, Å	14.415(3)	10.654(2)	11.150(2)	12.832(4)	15.607(3)	14.528(4)
b, Å	14.838(4)	11.278(2)	14.369(2)	26.449(8)	15.394(2)	19.545(4)
c, Å	16.015(4)	12.065(2)	15.683(2)	39.43(2)	8.740(2)	24.525(6)
α, deg	90	100.578(4)	87.979(3)	90	90	90
β, deg	90	96.673(4)	69.464(2)	90	90	103.177(5)
γ, deg	90	94.580(4)	78.575(3)	90	90	90
V, Å^3	3425(2)	1407.7(5)	2304.6(5)	13381(7)	2099.7(6)	6780(3)
Z	4	1	2	8	4	4
T (K)	213	213	193	213	193	213
ρ_{calc}, g cm^{-3}	1.203	1.185	1.478	1.595	1.630	1.573
2θ range, deg	3.74−45.00	3.46−45.00	2.78−45.00	2.98−50.00	5.96−50.00	3.42−45.00
GOF (F^2)	1.042	1.126	0.821	1.029	1.170	0.600
R_1[b]/wR_2[c]	0.0300/0.0721	0.0480/0.1283	0.0332/0.0667	0.0678/0.1540	0.0642/0.1668	0.0445/0.0600

	[**7**]·CH_3CN	[**8**]	[**9**]	[**10**]$(PF_6)_2$·2CH_3CN	[**11**]	[**12**]
formula	$C_{30}H_{59}Cl_4N_5Ni_2S_4Zn_2$	$C_{17}H_{35}Cl_2N_3NiOS_2Zn$	$C_{14}H_{28}Cl_2HgN_2NiS_2$	$C_{42}H_{78}Cu_2F_{12}N_6Ni_3P_2S_6$	$C_{62}H_{68}Cu_2N_2NiO_2P_2S_2$	$C_{39}H_{48}CuN_2NiOPS_3$
cryst syst	monoclinic	monoclinic	monoclinic	monoclinic	monoclinic	triclinic
fw	1008.02	556.58	618.70	1452.61	1185.03	810.19
space group	$P2_1/n$	$P2_1/c$	$C2/c$	$P2_1/c$	Cc	$P\bar{1}$
a, Å	17.464(7)	16.141(3)	25.09(3)	43.028(9)	17.317(2)	9.670(1)
b, Å	12.284(5)	18.000(4)	15.98(2)	11.992(3)	13.405(2)	11.307(2)
c, Å	20.244(8)	8.325(2)	22.52(3)	26.633(5)	24.843(3)	18.285(2)
α, deg	90	90	90	90	90	91.598(2)
β, deg	93.51(2)	90.930(4)	97.13(2)	95.998(4)	95.119(2)	95.614(2)
γ, deg	90	90	90	90	90	105.560(2)
V, Å^3	4343(3)	2418.5(9)	8963(18)	13668(5)	5744(1)	1913.7(3)
Z	4	4	16	8	4	2
T (K)	193	193	193	193	213	213
ρ_{calc}, g cm^{-3}	1.542	1.529	1.834	1.412	1.370	1.406
2θ range, deg	3.10−45.00	2.52−56.56	3.02−45.00	3.32−45.00	3.30−45.00	3.74−56.00
GOF (F^2)	0.869	0.901	0.989	1.084	1.011	1.039
R_1[b]/wR_2[c]	0.0493/0.0843	0.0324/0.0724	0.0430/0.1124	0.0980/0.2580	0.0495/0.0960	0.0424/0.0954

[a] Mo Kα radiation. [b] $R_1 = \sum||F_o| - |F_c||/\sum|F_o|$. [c] $wR_2 = \{\sum[w(F_o^2 - F_c^2)^2/\sum[w(F_o^2)^2]\}^{1/2}$.

In the sections that follow, complexes and one ligand are referred to by the numerical designations in Chart 1.

X-ray Structure Determinations. The 24 compounds listed in Tables 1 and 2 were structurally identified by X-ray crystallography. Suitable crystals were obtained by the following methods in which solutions were allowed to stand at room temperature for the indicated periods: (i) layering ether onto or vapor diffusion of ether into acetonitrile solutions (1−6 days) {$(Et_4N)_2$[**1**]·MeCN and $(Et_4N)_3$[**2**] (red blocks), $(Et_4N)_2$[**3**] and $(Et_4N)_3$[**4**]·1.5MeCN·0.5H_2O (orange-red blocks), [**7**]·MeCN (purple blocks), [**10**]$(PF_6)_2$·2MeCN and [**17**]$_3(PF_6)_6$·2MeCN·Et_2O (red blocks), **15** (pink needles), [**16**]$(OTf)_2$ (dark brown blocks), [**19**]$(PF_6)_2$·MeCN (dark brown plates), $(Et_4N)_2$[**23**] (green blocks), $(Et_4N)_2$[**24**] and **25** (red blocks), **26** (red-brown blocks), and $(Et_4N)_2$[**27**] (green blocks)}; (ii) vapor diffusion of ether into THF solutions (≥3 days) {[**5**]$Na(PF_6)$ (orange plates) and [**18**](PF_6)·THF (green-brown blocks)}; (iii) vapor diffusion of pentane into a THF solution (≥1 day) {[**6**]$(OTf)_2$·2Et_2O (pink blocks)} (iv) vapor diffusion of ether into DMF solutions (>2 days) {**7**, **8** (pink plates)}; (v) layering ether onto or vapor diffusion of ether into dichloromethane solutions (overnight) {**9** (pink blocks), **12** (brown blocks), and [**13**]·CH_2Cl_2 (purple plates)}; (vi) layering hexanes on a toluene solution (<1 day) {**11** (dark red blocks)}; (vii) layering ether onto an acetonitrile/dichloromethane solution (<1 day) {[**14**]·CH_3CN (purple needles)}. The crystals were coated in grease and mounted on a Siemens (Bruker) SMART CCD area detector instrument equipped with Mo Kα radiation. Data were collected at 193 or 213 K using ω scans of 0.3° per frame, with 10 s ($(Et_4N)_2$[**3**] and **12**), 20 s ([**6**]$(OTf)_2$·2Et_2O), 30 s ($(Et_4N)_2$[**1**]·MeCN, $(Et_4N)_3$[**2**], $(Et_4N)_3$[**4**]·1.5MeCN·0.5H_2O, [**7**]·MeCN, **8**, **9**, [**10**]$(PF_6)_2$·2MeCN, **11**, [**13**]·CH_2Cl_2, [**14**]·MeCN, **15**, [**16**]$(OTf)_2$, [**17**]$_3(PF_6)_6$·2MeCN·Et_2O, [**18**](PF_6)·THF, $(Et_4N)_2$[**24**], **25**, and $(Et_4N)_2$[**27**]), or 60 s ([**19**]$(PF_6)_2$·MeCN, $(Et_4N)_2$[**23**], and **26**) per frame, such that 1271 frames were collected for a hemisphere of data. The first 50 frames were re-collected at the end of the data collection to monitor for decay; no significant decay was detected for any compound. Data out to 2θ of 50.0° were used for $(Et_4N)_3$[**4**]·1.5MeCN·0.5H_2O and [**5**]$NaPF_6$ and out to 56.6° for **8**, **12**, [**18**](PF_6)·THF, and **26**; for the remaining compounds, data were used only out to 2θ of 45° because of the low-quality high-angle data. Cell parameters were retrieved using SMART software and refined using SAINT software on all observed reflections between 2θ of 3° and the upper thresholds. Data reduction was performed with SAINT software, which corrects for Lorentz polarization and decay. Absorption corrections were applied using SADABS, as described by Blessing.[40] The space groups for all of the compounds were assigned unambiguously by analysis of symmetry and systematic absences determined by XPREP. Crystal parameters are listed in Tables 1 and 2. All of the structures were solved by the direct method with SHELXS-97 and subsequently refined against all data in the 2θ ranges by full-matrix least squares on F^2 using SHELXL-97. All non-hydrogen atoms, including those of the disordered cations or disordered solvent molecules, were refined anisotropi-

(40) Blessing, R. H. *Acta Crystallogr.* **1995**, *A51*, 33−38.

Table 2. Crystallographic Data for Compounds Containing Complexes **13**−**19** and **23**−**27**[a]

	[**13**]·CH_2Cl_2	[**14**]·CH_3CN	[**15**]	[**16**]·$(OTF)_2$	[**17**]$_3(PF_6)_6$·$2CH_3CN$·Et_2O	[**18**](PF_6)·THF
formula	$C_{34}H_{50}Cl_2Cu$-N_3NiPS_2	$C_{34}H_{46}ClCu$-N_3NiPS_2	$C_{39}H_{50}Cu$-N_2NiPS_3	$C_{32}H_{59}F_6N_5$-$Ni_3O_6S_6$	$C_{74}H_{163}F_{36}N_{11}$-$Ni_6OP_{12}S_6$	$C_{36}H_{51}ClF_6$-$N_2Ni_2OP_2S_2$
cryst syst	monoclinic	monoclinic	orthorhombic	monoclinic	monoclinic	monoclinic
fw	789.01	749.53	796.21	1092.33	2823.40	920.72
space group	$P2_1/c$	$P2_1$	$Pna2_1$	$P2_1/n$	$P2_1/c$	$P2_1/n$
a, Å	23.099(3)	13.607(3)	22.609(4)	15.002(4)	11.343(2)	20.534(3)
b, Å	11.093(2)	10.894(3)	11.819(2)	12.281(3)	32.162(6)	9.730(2)
c, Å	29.246(4)	13.668(3)	14.498(2)	25.875(6)	34.020(6)	20.929(3)
α, deg	90	90	90	90.	90	90
β, deg	93.29(2)	115.574(5)	90	100.700(7)	98.829(4)	94.827(3)
γ, deg	90	90	90	90.	90	90
V, Å^3	7482(2)	1827.5(7)	3874(2)	4684(2)	12264(4)	4167(1)
Z	8	2	4	4	4	4
T (K)	213	193	193	193	193	193
ρ_{calc}, g cm^{-3}	1.401	1.362	1.365	1.549	1.529	1.468
2*θ* range, deg	3.22−45.00	3.52−45.00	3.60−45.00	3.20−45.00	3.64−45.00	3.90−56.64
GOF (F^2)	0.889	0.720	0.859	1.095	1.046	1.024
R_1[b]/wR_2[c]	0.0566/0.1272	0.0420/0.0641	0.0531/0.0808	0.0839/0.2444	0.0720/0.1845	0.0497/0.1469

	[**19**]$(PF_6)_2$·CH_3CN	$(Et_4N)_2$[**23**]	$(Et_4N)_2$[**24**]	[**25**]	[**26**]	$(Et_4N)_2$[**27**]
formula	$C_{44}H_{73}F_{12}$-$N_5Ni_4P_2S_6$	$C_{30}H_{60}N_6$-$Ni_3O_4S_4$	$C_{23}H_{50}N_4$-NiO_2S_2	$C_{17}H_{34}N_2$-$Ni_2O_2P_2S_2$	$C_{33}H_{34}N_2$-$Ni_2O_2P_2S_2$	$C_{30}H_{60}Cu$-$N_6Ni_2O_4S_4$
cryst syst	monoclinic	monoclinic	orthorhombic	monoclinic	orthorhombic	monoclinic
fw	1389.21	873.21	537.50	541.94	734.10	878.04
space group	$I2/m$	$P2_1/c$	$Aba2$	$P2_1/c$	$Pca2_1$	$P2_1/c$
a, Å	16.486(6)	12.306(5)	28.178(3)	9.399(2)	16.794(3)	12.326(2)
b, Å	24.609(9)	11.977(5)	13.648(2)	10.265(2)	10.248(2)	11.987(2)
c, Å	17.605(9)	12.837(5)	14.233(2)	23.662(5)	18.701(3)	12.867(2)
α, deg	90	90	90	90	90	90
β, deg	117.323(6)	93.825(7)	90	92.319(5)	90	93.512(4)
γ, deg	90	90	90	90	90	90
V, Å^3	6346(5)	1888(1)	5473(1)	2281.0(9)	3219(1)	1897.4(4)
Z	4	2	8	4	4	2
T (K)	193	213	193	193	193	213
ρ_{calc}, g cm^{-3}	1.454	1.536	1.305	1.578	1.515	1.537
2*θ* range, deg	2.80−45.00	3.32−45.00	2.90−45.00	3.44−45.00	3.98−56.74	3.32−45.00
GOF (F^2)	1.036	1.153	1.039	1.040	0.997	1.042
R_1[b]/wR_2[c]	0.0896/0.2526	0.0761/0.1565	0.0507/0.1376	0.0557/0.1494	0.0649/0.1199	0.0563/0.1257

[a] Mo Kα radiation. [b] $R_1 = \sum||F_o| - |F_c||/\sum|F_o|$. [c] $wR_2 = \{\sum[w(F_o^2 - F_c^2)^2/\sum[w(F_o^2)^2]\}^{1/2}$.

cally. Hydrogen atoms were attached at idealized positions on carbon atoms and were checked for missing symmetry by the program PLATON.

One of the three cations of $(Et_4N)_3$[**2**] is disordered because the nitrogen atom appeared at the inversion center; thus, hydrogen atoms are omitted for this cation. The solvent molecules in $(Et_4N)_3$-[**4**]·1.5MeCN·0.5H_2O, [**10**]$(PF_6)_2$·2MeCN, [**14**]·MeCN, [**17**]$_3(PF_6)_6$·2MeCN·Et_2O, and [**19**]$(PF_6)_2$·MeCN are disordered. Apparently, because of the asymmetric nature of the ligand, the anion of $(Et_4N)_2$-[**24**] was disordered over two overlapping positions superimposed at the nickel atom. The structure was solved and refined in orthorhombic space group *Aba*2 with 65% and 35% occupancies of the two orientations. Final agreement factors for all structures are given in Tables 1 and 2.[41] The compound [**5**]·$NaPF_6$ was solved in C-centered orthorhombic space group $Cmc2_1$. The anion is located on a crystallographic mirror plane; some carbon atoms display elongated thermal ellipsoids along the *c*-axis.

Other Physical Measurements. All measurements were performed under anaerobic conditions. ^{1}H NMR spectra were measured with a Varian AM-400B spectrometer. Cyclic voltammograms (100 mV/s) were recorded with a Princeton Applied Research model 263 potentiostat/galvanostat using a Pt working electrode and 0.1 M $(Bu_4N)(PF_6)$ supporting electrolyte. Potentials are referenced to an SCE. Electrospray mass spectra were recorded on a Platform II quadrupole mass spectrometer (Micromass Instruments, Danvers, MA) or on an LCT-TOF mass spectrometer (Micromass Instruments, Danvers, MA). Absorption spectra were recorded with a Cary 3 spectrophotometer.

(41) See paragraph at the end of this article for Supporting Information available.

Results and Discussion

The A-cluster bridges in Figure 1 raise the general question of the types of bridges that can be sustained by binding to the sulfur atoms of a cis-planar $Ni^{II}-S_2N_2$ distal site. Our considerations start with this matter, which is step ii in the three steps to achieving an A-cluster analogue. Two complexes derived from tetradentate ligands, anionic $[Ni(L_H\text{-}S_2N_2)]^{2-}$ (**1**), first synthesized in this laboratory,[30] and neutral $[Ni(L_R\text{-}S_2N_2)]$ (**5**), prepared by Schugar and co-workers,[31] were first selected for exploration of bridge formation. A similar approach with different molecules has been taken by others.[14−18] Complex **5** was examined more extensively. Subsequently, we introduce $[Ni(L\text{-}655)]^{2-}$ (**24**), a physiologically realistic diamidodithiolate representation of the distal nickel binding site in A-clusters. These are template molecules upon which Ni−S−M bridging interactions of various types are built. The intent of this work is to disclose (at least some of the) bridging modes of $Ni^{II}-S_2N_2$ species with, primarily, M = Cu^I, Zn^{II}, and Ni^{II}. Because binuclear bridged molecules were anticipated, reactions were generally

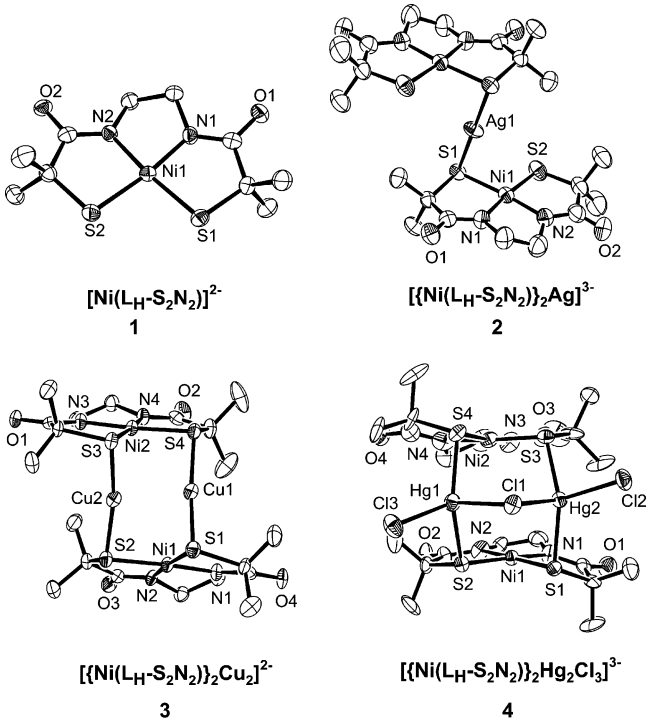

Figure 2. Structures of mononuclear **1** and bridged complexes **2**−**4** derived therefrom. $[Ni(L_H\text{-}S_2N_2)]^{2-}$ (**1**): Ni−S 2.181(1), Ni−N 1.858(2), N−Ni−N 85.67(9), N(1)−Ni−S(1) 87.61(7), N(2)−Ni−S(2) 87.71(7), S−Ni−S 99.10(3). $[\{Ni(L_H\text{-}S_2N_2)\}_2Ag]^{3-}$ (**2**, *i*): Ni−S(1) 2.191(2), Ni−S(2) 2.157(2), Ni−N 1.86(1), Ni−Ag 3.006(1), S−Ag−S 180, Ni−S−Ag 82.02(5). $[\{Ni(L_H\text{-}S_2N_2)\}_2Cu_2]^{2-}$ (**3**): Ni−S 2.182(1), Ni−N 1.854(3), Cu−S 2.173(1), Cu−Cu 2.644(1), S−Ni−S 98.5(7), S−Cu−S 167(1), S−Cu−Cu 93.64(4), Ni−S−Cu 77.61(4)−92.75(4). $[\{Ni(L_H\text{-}S_2N_2)\}_2Hg_2Cl_3]^{3-}$ (**4**, 2 inequiv): Ni−S 2.18(1), Ni−N 1.857(9), Hg−S 2.441(4), Hg−Cl 2.623(4), Hg−μ_2Cl 2.754(4), S−Hg−S 147.2(1), Ni−S−Hg 98.3(2), Hg−μ_2Cl−Hg 86.5(1), Cl−Hg−μ_2Cl 102(1). In this and succeeding figures, 50% probability ellipsoids, partial atom labeling schemes, crystallographically imposed symmetry elements, and the number of complexes (>1) in the asymmetric unit are given; selected (mean) bond lengths (Å) and angles (deg) are summarized with standard deviations from the mean as appropriate. When more than one inequivalent complex is present, metric differences are small and distances and angles refer to one complex only.

performed in acetonitrile with an ca. 1:l mol ratio of reactants. Complexes that were isolated were those that crystallized under the specified experimental conditions. Reaction products were characterized by electrospray mass spectrometry and crystal structure determinations of some 24 species. Except for **24** and related complexes, other properties were not sought because the thrust of this research is structural. It was sometimes not possible to isolate crystalline products from reaction of each Ni^{II} complex with same reactant, thereby eliminating certain direct comparisons of structure. Bridging modes other than those described here might result from variant experimental conditions, including reaction stoichiometry and different reactants. Because of the large quantity of data, structural information has been condensed to the depictions and the parameters in Figures 2−8 and Tables 3−6.[41]

Complexes Derived from $[Ni(L_H\text{-}S_2N_2)]^{2-}$. Dianionic complex **1** (Figure 2) is one in a set of species containing tetradeprotonated amidate−thiolate ligands that stabilize the Ni^{III} state at unusually low potentials.[30,42] It is planar with a 5−5−5 pattern of chelate rings, Ni−S = 2.181(1) Å, Ni−N = 1.858(2) Å, and S−Ni−S = 99.10(3)°. Reactions are summarized in Scheme 1; structures of bridged products are provided in Figure 2. Two Cu^{I} reactants afford the doubly bridged assembly **3**, consisting of two units **1** canted in a cisoid arrangement with dihedral angle $\chi = 147°$ between the $Ni-S_2N_2$ mean planes, four Ni−(μ_2-S)−Cu bridges, and two nearly linear S−Cu−S interactions (167°). Reaction of **1** with two other thiophiles, M = Ag^{I} and Hg^{II}, leads to **2** and **4**, respectively. Both resemble **3** by having Ni−(μ_2-S)−M bridges and S−M−S links between units **1**. Centrosymmetric **2** has two Ni−(μ_2-S)−Ag bridges and a linear S−Ag−S bridge. Complex **4** shows four Ni−(μ_2-S)−Hg bridges, two roughly parallel cisoid units **1** ($\chi = 167°, 172°$), and two nonlinear S−Hg−S links (S−Hg−S 147°) with highly distorted tetrahedral coordination at the mercury atoms. Double S−Cu^{I}−S bridging has been observed in two other assemblies analogous to **3**.[14,15] In one instance, treatment of an assembly with PR_3 (R = Pr^i, NMe_2) resulted in bridge cleavage and formation of a nonplanar bridging Ni-(μ_2-S)$_2$Cu rhomb,[15] a structural unit of significance in step ii (vide infra).

Scheme 1. Preparations and Schematic Structures of Ag^{I}-Bridged (**2**), Cu^{I}-Bridged (**3**), and Hg^{II}-Bridged (**4**) Complexes Derived from $[Ni(L_H\text{-}S_2N_2)]^{2-}$ (**1**)

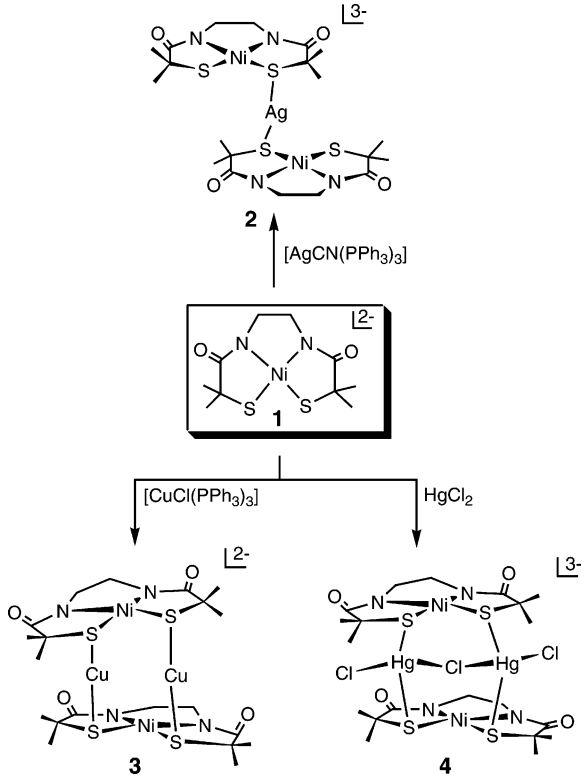

Complexes Derived from $[Ni(L_R\text{-}S_2N_2)]$. Neutral complex **5** (Figure 3) is essentially planar and, with a 5−5−5 ring pattern, resembles **1** but with shorter Ni−S bonds (2.158(2) Å), longer Ni−N bonds (1.923(7) Å), and a smaller S−Ni−S angle (94.21(9)°). Complexes are classified as nonrhombic or rhombic, depending upon whether they contain the structural element Ni(μ_2-S)$_2$M.

(1) Nonrhombic. (a) Zn^{II}- and Hg^{II}-Bridged. Reactions are set out in Scheme 2; structures of three Zn^{II}-bridged

(42) Krüger, H.-J.; Holm, R. H. *Inorg. Chem.* **1987**, *26*, 3645−3647.

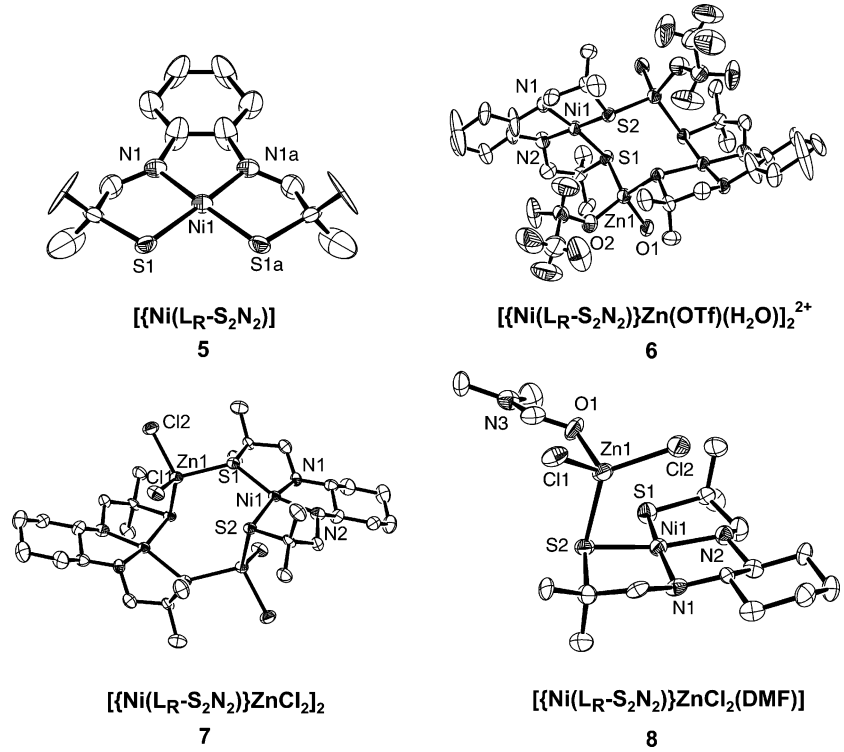

Figure 3. Structures of **5** and of Zn^{II}-bridged complexes **6**−**8** derived therefrom. [$Ni(L_R\text{-}S_2N_2)$] (**5**): Ni−S 2.158(2), Ni−N 1.923(7), N−Ni−N 86.5(4), N−Ni−S 89.6(2), S−Ni−S 94.21(9). [{$Ni(L_R\text{-}S_2N_2)$}$Zn(OTf)(H_2O)]_2^{2+}$ (**6**, *i*): Ni−S 2.159(3), Ni−N 1.92(2), Zn−S 2.321(2): Zn−O(H_2O) 1.937(7), Zn−OTf 2.019(6), Ni−S−Zn 109.2(1) and S−Zn−S 111.6(1). [{$Ni(L_R\text{-}S_2N_2)$}$_2ZnCl_2]_2$ (**7**, *i*, 2 inequiv): Ni−S 2.179(3), Ni−N 1.933(6), Zn−S 2.383(2), Zn−Cl 2.294(1), S−Ni−S 98.05(8), Ni−S(1)−Zn 127.65(9), Ni−S(2)−Zn 87.40(7). [{$Ni(L_R\text{-}S_2N_2)$}$ZnCl_2$(DMF)] (**8**): Ni−S(1) 2.141(1), Ni−S(2) 2.159(1), Ni−N 1.94(2), Zn−S 2.356(1), S−Ni−S 95.55(3), Ni−S−Zn 84.47(3), Cl(1)−Zn−S 111.23(3), Cl(2)−Zn−S 123.92(3), Cl−Zn−Cl 108.20(3).

Scheme 2. Preparations and Schematic Structures of Zn^{II}-Bridged (**6**−**8**) and Hg^{II}-Bridged (**9**) Complexes Derived from [$Ni(L_R\text{-}S_2N_2)$] (**5**)

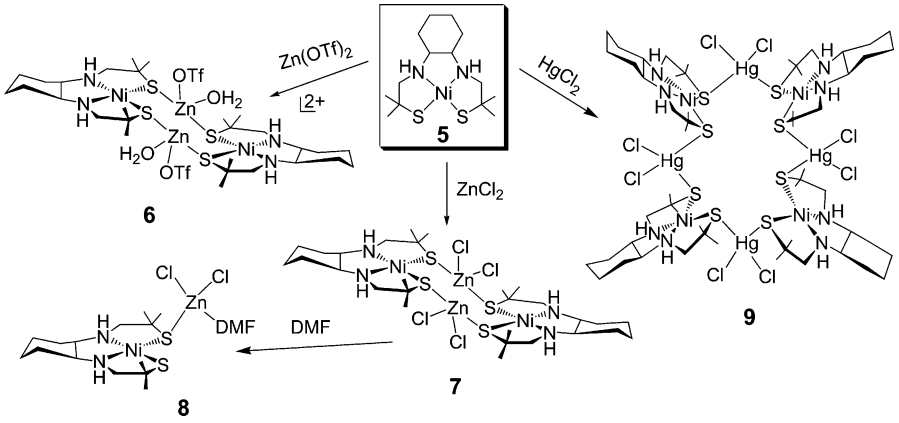

products are presented in Figure 3, and there is one Hg^{II} complex in Figure 4. Reaction of **5** with $Zn(OTf)_2$ yielded centrosymmetric complex **6**, which incorporates two units **5** joined by two S−Zn−S links implicating four Ni−(μ_2-S)−Zn bridges. The bridges are nonlinear (S−Zn−S = 111.6(1)°, Ni−S−Zn 106.6(1)°, 111.7(1)°) with the zinc atoms displaying distorted tetrahedral stereochemistry. Use of $ZnCl_2$ afforded **7**, also centrosymmetric, whose relationship to **6** is obvious. When **7** was recrystallized from DMF, binuclear **8** was formed containing a Ni−(μ_2-S)−Zn bridge (Ni−S−Zn = 84.47(3)°). Treatment of **5** with $HgCl_2$ gave cyclic octanuclear **9**, incorporating four units **5** each of which is connected to other units through binding to $HgCl_2$. The resulting structure has D_2 symmetry with four independent Ni−(μ_2-S)−Hg and two independent S−Hg−S bridges. We are unaware of any precedents of structures **6**−**9**. Previously, a pentanuclear complex has been isolated in which three Ni−S_2N_2 complexes are connected by two zinc centers via six S−Zn−S bridges in a structure approaching C_3 symmetry.[43]

(b) Cu^I-Bridged. Reactions are depicted in Scheme 3; structures of six bridged species are provided in Figures 4 and 5. Pentanuclear complex **10** results from the reaction of **5** and $[Cu(MeCN)_4]^{1+}$ in which all acetonitrile ligands are displaced. Its trigonally symmetric structure involves two copper atoms, each of which binds one sulfur atom of three units **5**. Over two independent molecules, the mean S−Cu−S angle is 120(3)°, the range of the 12 Ni−(μ_2-S)−Cu angles is 82.3(1)−101.3(1)°, and χ = 119−121°. The Cu···Cu

(43) Tuntulani, T.; Reibenspies, J. H.; Farmer, P. J.; Darensbourg, M. Y. *Inorg. Chem.* **1992**, *31*, 3497−3499.

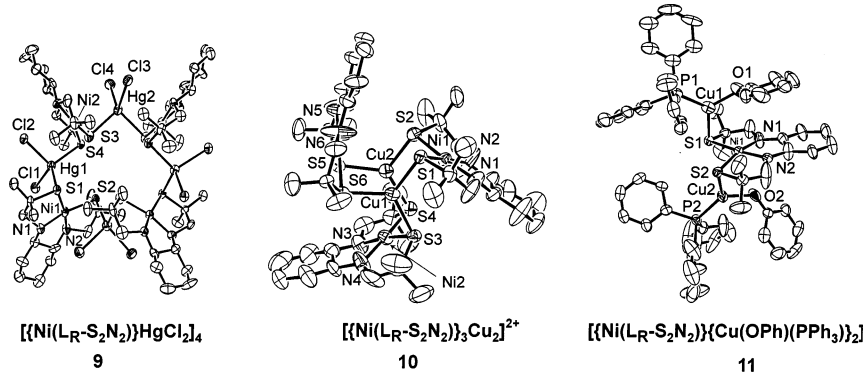

Figure 4. Structures of Hg^{II}-bridged (**9**) and Cu^{I}-bridged (**10**, **11**) complexes derived from $[Ni(L_R\text{-}S_2N_2)]$ (**5**). $[\{Ni(L_R\text{-}S_2N_2)\}HgCl_2]_4$ (**9**, $3C_2$): Ni−S 2.17(1), Ni−N 1.95(1), Hg−S 2.527(2), Hg−Cl 2.56(3), S−Ni−S 96.7(6), Ni−S−Hg 83.0(1)−86.1(2), S(1)−Hg(1)−S(4) 118.4(1), S(2′)−Hg−S(3) 96.4(2). $[\{Ni(L_R\text{-}S_2N_2)\}_3Cu_2]^{2+}$ (**10**, 2 inequiv): Ni−S 2.158(4), Ni−N 1.90(3), Cu−S 2.294(8), Cu−Cu 3.099(2), S−Ni−S 96.8(5), S−Cu−S 116.6(1)−124.1(1), Ni−S−Cu 83.1(1)−100.8(1). $[\{Ni(L_R\text{-}S_2N_2)\}-\{Cu(OPh)(PPh_3)\}_2]$ (**11**): Ni−S 2.170(7), Ni−N 1.91(2), Cu−S 2.30(2), Cu−P 2.21(1), P(1)−Cu−S(1) 124.83(9), P(2)−Cu−S(2) 127.28(8), S−Ni−S 95.72(8), Ni−S(1)−Cu(1) 83.52(8), Ni−S(2)−Cu(2) 74.55(7).

Scheme 3. Preparations and Schematic Structures of Cu^{I}-Bridged Complexes (**10**−**15**) Derived from $[Ni(L_R\text{-}S_2N_2)]$ (**5**)

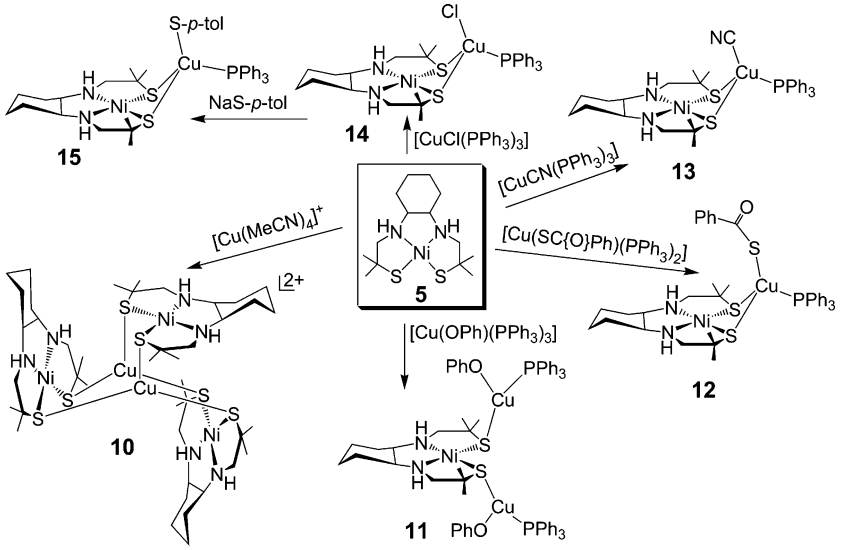

distance (3.099(2) Å) is nonbonding. A similar trigonal $M_2(Ni{-}S_2N_2)_3$ motif has been observed in complexes with M = Zn^{II},[16] and Cu^{I}.[14,16] With the less labile reactant $[Cu(OPh)(PPh_3)_3]$, complex **11** is formed with two anti Ni−(μ_2-S)−Cu bridges (74.55(7)° and 83.52(8)°) in which each copper atom retains two ligands. The bridging interactions are quite similar to those in **8**.

(2) Rhombic. Up to this point, all complexes **2**−**4** and **6**−**11** have been shown to sustain bridging interactions in which the sulfur atoms of templates **1** and **5** each bind to a different metal atom in the bridges of the type Ni−(μ_2-S)−M. Hereafter, we encounter molecules (with one exception) in which the bridging interactions take the form of nonplanar Ni(μ_2-S)$_2$M rhombs, which are the operative bridge units in A-clusters (Figure 1). The structures of complexes containing this feature are shown in Figures 5 and 6; metric properties of the rhombs are summarized in Tables 3 and 4.

(a) Cu^{I}-Bridged. Reaction of three Cu^{I} species with anionic ligands resulted in the formation of **12**−**14** (Scheme 3, Figure 5) containing Ni(μ_2-S)$_2$Cu bridging rhombs and retention of the ligand anion and one Ph_3P at the tetrahedral Cu^{I} sites. The structure of the NiS_2 portion is barely perturbed relative to free **5**, as is the case in practically all nonrhomb- and rhomb-bridged species. The rhombs are unsymmetrical with Cu−S distances within a molecule differing by 0.12−0.25 Å and are folded along the S···S diagonal with dihedral angles of 99−105°. The reaction of **14** with 1 equiv of Na(S-*p*-tol) in acetonitrile resulted in terminal ligand substitution, rather than bridge opening, to give **15**.

(b) Ni^{II}-Bridged. As shown in Scheme 4, treatment of **5** with five Ni^{II} complexes ranging from labile paramagnetic to planar diamagnetic species results in formation of **16**−**18**, **20**, and **21**. Structures of **16**−**19** are given in Figure 6. Use of $Ni(OTf)_2$ gave trinuclear **16**, containing one bridge rhomb and two units of **5**, one of which binds to the central planar nickel atom through a Ni−(μ_2-S)−Ni bridge (Ni−S−Ni = 95.2(2)°). Complex **17** contains one such bridge with Ni−S−Ni = 89.6(1)−91.2(1)° and a distorted tetrahedral nickel site. The overall structure resembles **8**. Reaction of **18** with Na_2(nbt) ruptured the bridge to afford **5**, which was isolated from acetonitrile/ether as diffraction-quality crystals of [**5**]·$NaPF_6$. This allowed the first structure determination of the complex; $[Ni_4(nbt)_8]$[44] was identified as a reaction product by an X-ray structure. Treatment of

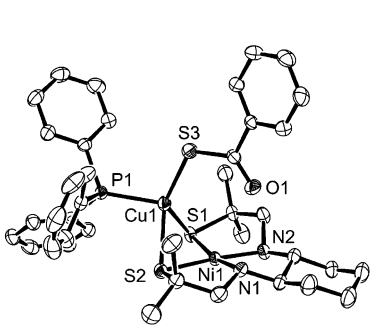

[{Ni(L_R-S_2N_2)}Cu(SC{O}Ph)(PPh_3)]

12

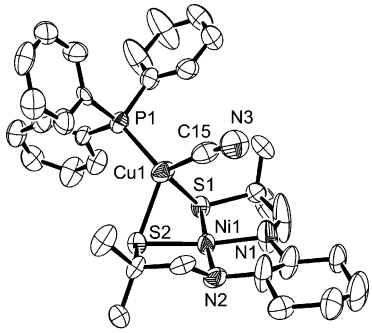

[{Ni(L_R-S_2N_2)}CuCN(PPh_3)]

13

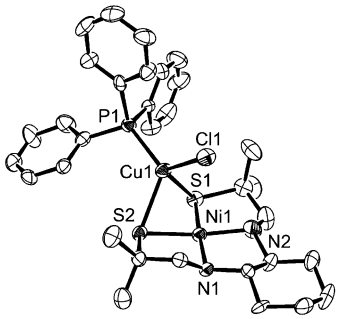

[{Ni(L_R-S_2N_2)}CuCl(PPh_3)]

14

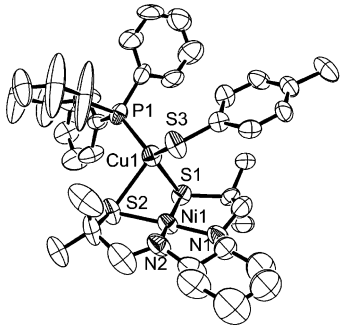

[{Ni(L_R-S_2N_2)}Cu(S-*p*-Tol)(PPh_3)]

15

Figure 5. Structures of Cu^{I}-bridged complexes **12**, **13** (2 inequiv), **14**, and **15** derived from [Ni(L_R-S_2N_2)] (**5**). Each complex contains a nonplanar NiS_2Cu bridging rhomb.

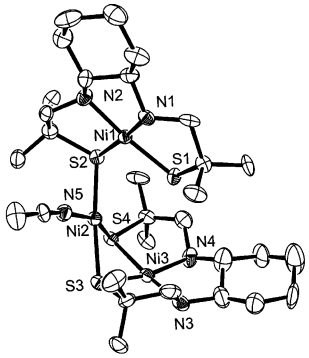

[{Ni(L_R-S_2N_2)}Ni(CH_3CN){Ni(L_R-S_2N_2)}]$^{2+}$

16

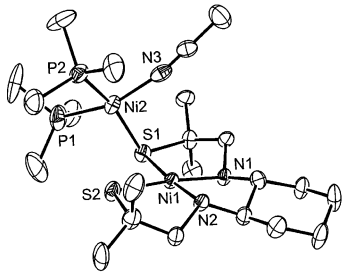

[{Ni(L_R-S_2N_2)}Ni(PMe_3)$_2$(CH_3CN)]$^{2+}$

17

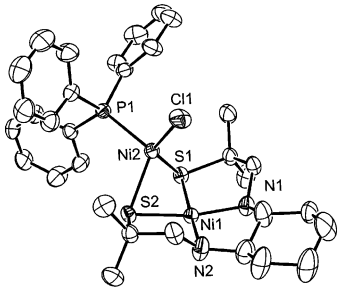

[{Ni(L_R-S_2N_2)}Ni(PPh_3)Cl]$^{1+}$

18

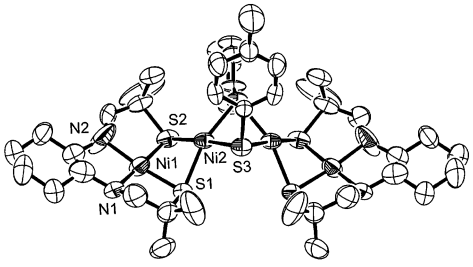

[{Ni(L_R-S_2N_2)}Ni(S-*p*-tol)]$_2^{2+}$

19

Figure 6. Structures of Ni^{II}-bridged complexes **16**−**19** derived from [Ni(L_R-S_2N_2)] (**5**). Complexes **16**, **18**, and **19** (C_2) contain nonplanar NiS_2Ni bridging rhombs; complex **17** contains one Ni−(μ_2-S)−Ni bridge. [{Ni(L_R-S_2N_2)}Ni(PMe_3)$_2$(MeCN)]$^{2+}$ (**17**, 3 inequiv): Ni(1)−S(1) 2.157(5), Ni(1)−S(2) 2.150(5), Ni−N 1.93(2), Ni(2)−S 2.232(2), Ni−P 2.18(2), Ni(2)−N 1.909(9), S(1)−Ni−S(2) 94.43(9), Ni−S(1)−Ni 91.24(9), S−Ni−P(1) 86.4(1), S−Ni−P(2) 159.7(1), S−Ni(2)−N 97.7(2).

Scheme 4. Preparations and Schematic Structures of Ni^{II}-Bridged Complexes (**16**−**21**) Derived from [$Ni(L_R$-S_2N_2)] (**5**)[a]

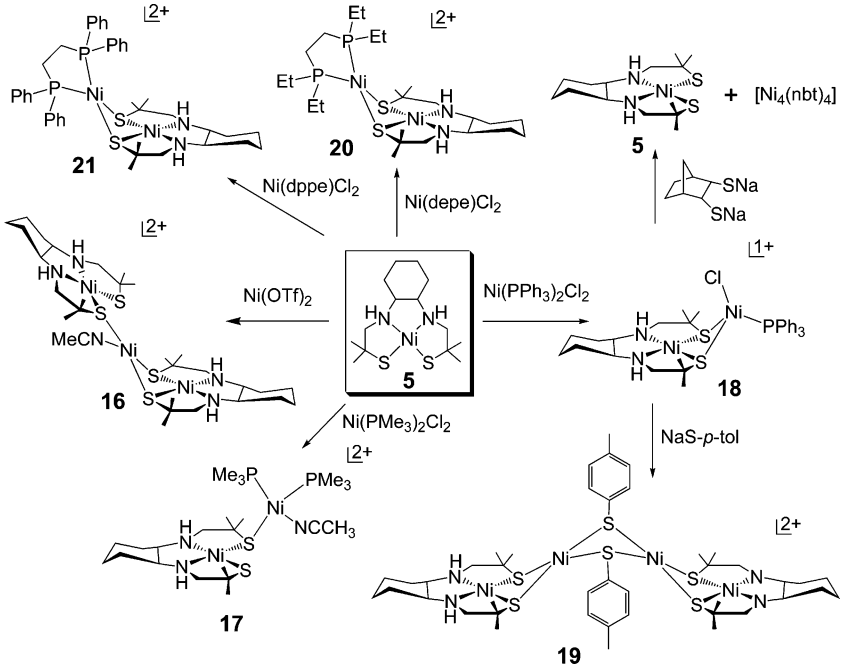

[a] Note the formation of **5** from **18**.

Table 3. Bond Distances (Å) of Complexes **12**−**16**, **18**, and **19**

	Ni−S(1)[a]	Ni−S(2)[a]	M−S(1)[a]	M−S(2)[a]	M−L(1)	M−L(2)[b]	Ni−M
12	2.175(1)	2.156(1)	2.397(1)	2.519(1)	2.276(1)	2.274(1)	2.658(1)
13	2.166(3)	2.172(3)	2.609(3)	2.361(3)	1.94(1)	2.233(3)	2.620(2)
14	2.156(2)	2.166(2)	2.522(2)	2.397(2)	2.328(2)	2.227(2)	2.644(1)
15	2.164(2)	2.155(2)	2.412(2)	2.560(2)	2.297(2)	2.236(2)	2.601(1)
16[c]	2.143(4)	2.130(4)	2.252(4)	2.234(4)	2.222(4)	1.89(1)	2.870(2)
18	2.161(1)	2.168(1)	2.306(1)	2.298(1)	2.193(1)	2.272(1)	2.591(1)
19	2.112(4)	2.118(4)	2.249(4)	2.235(4)	2.208(4)	2.196(4)	2.848(3)

[a] Bridging rhomb, M = Cu^I, Ni^{II}. [b] L = Ph_3P, CN^-, Cl^-, MeCN, RS^-. [c] S(3,4).

Table 4. Bond Angles (deg)[a] of Complexes **12**−**16**, **18**, and **19**

	S−Ni−S	Ni−S(1)−M	Ni−S(2)−M	S−M−S	NiSS/MSS[b]	$M_{geometry}$[c]
12	94.43(3)	70.90(2)	68.80(2)	80.54(2)	104.50(3)	t
13	93.6(1)	65.78(8)	70.46(9)	78.84(9)	99.78(9)	t
14	93.97(8)	68.31(6)	70.60(6)	79.89(6)	103.09(7)	t
15	93.75(9)	69.06(6)	66.32(6)	78.63(7)	98.98(8)	t
16	84.7(1)	81.5(1)	82.2(1)	79.8(1)	120.7(1)	p
18	89.37(3)	70.81(3)	70.84(2)	82.80(3)	104.84(3)	t
19	87.9(2)	81.5(2)	81.7(2)	81.8(2)	124.4(1)	p

[a] Bridging rhomb, M = Cu^I, Ni^{II}. [b] Dihedral angle. [c] p = planar, t = (distorted) tetrahedral.

18 with Na(S-*p*-tol) also resulted in bridge cleavage and the formation of tetranuclear **19** containing three $Ni_2(\mu_2$-$S)_2$ rhombs. Apparently, the Ni_4 arrangement as $Ni_4(\mu_2$-$SR)_6$ has been found only as a portion of acyclic penta-[45,46] and hexanuclear[24] complexes. It is otherwise known in *cyclo*-$[Ni_4(SR)_8]$.[44,47−49] X-ray structures of diphosphine complexes

Scheme 5. Synthesis of the Diamidodithiol H_4(L-655) (**22g**)[a]

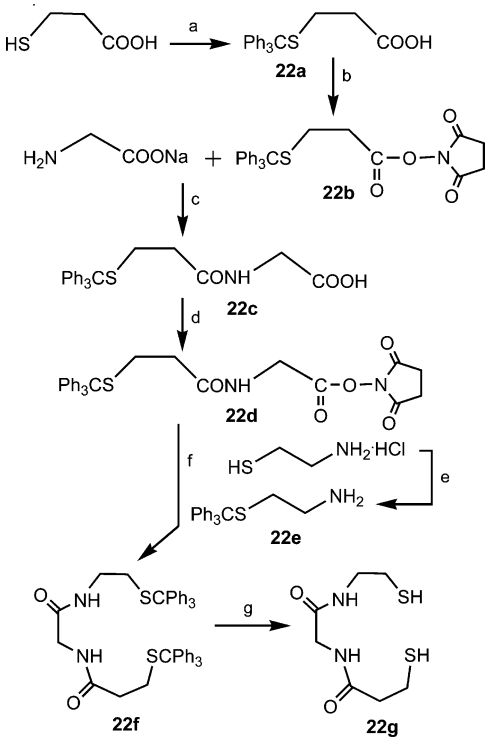

[a] Reaction conditions: a = Ph_3COH, $BF_3(OEt_2)$, HOAc, 75 °C; b = *N*-hydroxysuccinimide, dicyclohexylcarbodiimide, $MeOCH_2CH_2OMe$, −5 °C; c = glycine, $NaHCO_3$, $MeOCH_2CH_2OMe/DMF/H_2O$, −10 °C; d = *N*-hydroxysuccinimide, dicyclohexylcarbodiimide, $MeOCH_2CH_2OMe$, 0 °C, aq NaOH; e = Ph_3COH, CF_3COOH; f = CH_2Cl_2, 0 °C; g = Et_3SiH, CF_3COOH.

20 and **21** were not determined. Those shown (Scheme 4) are proposed by analogy to one (dppe)Ni−S_2N_2 species[17] and complexes **25** and **26** (see below).

[Ni(L-655)]$^{2-}$ and Bridged Derivatives. Having established an array of bridging modes based on Ni−S_2N_2

(44) Köckerling, M.; Henkel, G. *Inorg. Chem. Commun.* **2000**, *3*, 117−119.
(45) Sheng, T.; Zhang, W.; Wang, Q.; Gao, X.; Lin, P. *Chem. Commun.* **1998**, 263−264.
(46) Wang, Q.; Marr, A. C.; Blake, A. J.; Wilson, C.; Schröder, M. *Chem. Commun.* **2003**, 2776−2777.
(47) Gaete, W.; Ros, J.; Solans, X.; Font-Altaba, M.; Briansó, J. L. *Inorg. Chem.* **1984**, *23*, 39−43.
(48) Krüger, T.; Krebs, B.; Henkel, G. *Angew. Chem., Int. Ed. Engl.* **1989**, *28*, 61−62.

Scheme 6. Preparation of $[\{Ni(L\text{-}655)\}_2Ni]^{2-}$ (**23**) and $[Ni(L\text{-}655)]^{2-}$ (**24**) from H_4(L-655) (**22g**) and Ni^{II} Bridging Reactions of **24** to Afford **25**−**27**[a]

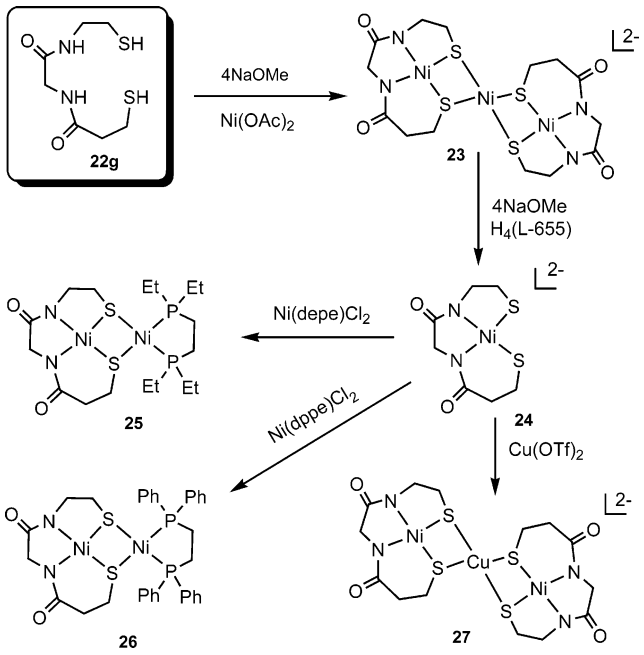

[a] All reactions were conducted in methanol/acetonitrile, and anionic complexes were isolated as Et_4N^+ salts.

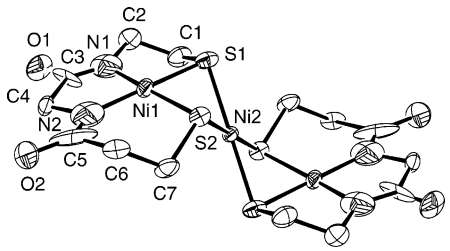

$[\{Ni(L\text{-}655)\}_2Ni]^{2-}$
23

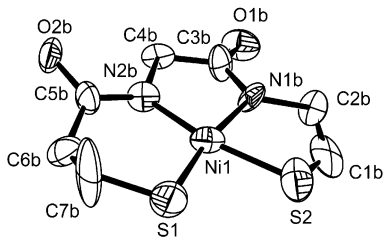

$[Ni(L\text{-}655)]^{2-}$
24

Figure 7. Structures of **23** (*i*, two nonplanar bridging rhombs) and **24** as Et_4N^+ salts. $[Ni(L\text{-}655)]^{2-}$ (**24**): Ni−S(1) 2.161(2), Ni−S(2) 2.191(2), Ni−N(1b) 1.941(5), Ni−N(2b) 1.854(5), S(1)−Ni−S(2) 89.05(6), S(1)−Ni−N(2b) 104.7(2), S(2)−Ni−N(1b) 81.6(2), N(1b)−Ni−N(2b) 84.8(2), S(1)−Ni−N(1b) 170.5(2), S(2)−Ni−N(2b) 166.2(2). The structure of the majority disordered form (65%) of **24** is depicted.

complexes **1** and **5**, we next examine the bridging propensity of a more accurate representation of the distal nickel site in A-clusters. The approach utilizes the diamidodithiol H_4(L-655) (**22g**). It is prepared in 26% yield from **22a** in a six-step synthesis, adapted from that of a related diamidodithiol (Scheme 5).[38] The deprotonated form of **22g** develops the 6−5−5 chelate ring pattern of the Cys-Gly-Cys protein sequence and differs compositionally from the native ligand only by lacking ring amido substituents which are part of the peptide chain. The simpler structure is intended to promote crystallization. The synthesis of Ni^{II} complexes and several bridging reactions are shown in Scheme 6. Structures are presented in Figures 7 and 8, and selected metric data are found in Tables 5 and 6.

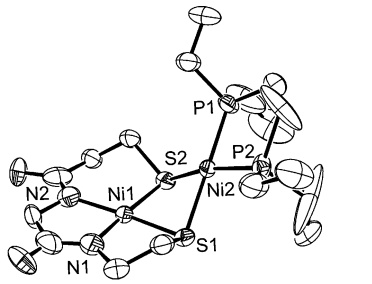

$[\{Ni(L\text{-}655)\}Ni(depe)]$
25

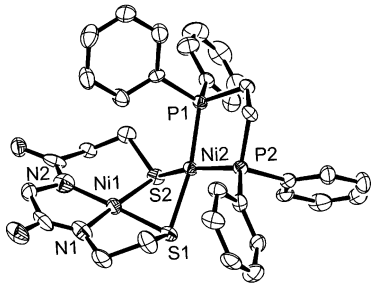

$[\{Ni(L\text{-}655)\}Ni(dppe)]$
26

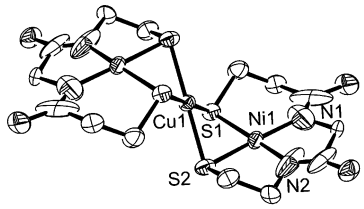

$[\{Ni(L\text{-}655)\}_2Cu]^{2-}$
27

Figure 8. Structures of bridged complexes **25**, **26**, and **27** derived from $[Ni(L\text{-}655)]^{2-}$ (**24**). Each complex contains a nonplanar NiS_2Ni or NiS_2Cu bridging rhomb.

Table 5. Bond Distances (Å) of Protein-Bound A-Clusters[a] and L-655 Complexes

	Ni−S(1)[b]	Ni−S(2)[b]	M−S(1)[b]	M−S(2)[b]	M−L[c]	M−L[c]	Ni−M
NiNi	2.25	2.22	2.14	2.35	2.34	2.38	3.04
NiCu	2.14	2.21	2.09	2.35	2.16	1.95	2.81
NiZn	2.20	2.24	2.34	2.34	2.37	2.28	2.83
23	2.153(3)	2.149(3)	2.204(2)	2.204(2)	2.204(2)	2.204(2)	2.757(2)
27	2.156(2)	2.159(2)	2.235(2)	2.239(2)	2.235(3)	2.239(3)	2.748(1)
25	2.151(2)	2.145(2)	2.248(2)	2.226(2)	2.158(2)	2.179(2)	2.925(1)
26	2.154(2)	2.149(2)	2.238(2)	2.216(2)	2.161(2)	2.167(2)	2.815(1)

[a] Data calculated from crystallographic coordinates.[8,9] [b] Bridging rhomb: M = Ni for **23**, **25**, and **26**; M = Cu for **27**. [c] L = S for **23** and **27**, L = P for **25** and **26**.

(49) Krüger, T.; Krebs, B.; Henkel, G. *Angew. Chem., Int. Ed. Engl.* **1992**, *31*, 54−56.

Table 6. Bond Angles (deg) of Protein-Bound A-Clusters and L-655 Complexes[a]

	S−Ni−S[b]	Ni−S−M[b]	Ni−S−M[b]	S−M−S[b]	S−Ni−N[c]	NiSS/MSS[d]	$M_{geometry}$[e]
NiNi	87	83	88	87	105	138	p
NiCu	85	77	81	83	95	118	t
NiZn	87	76	77	82	99	114	t
23	83.6(1)	78.48(9)	78.58(9)	81.18(9)	103.2(5)	114.5(2)	p
27	84.41(7)	77.33(7)	77.47(6)	80.75(7)	102.7(4)	112.6(1)	p
25	85.31(7)	83.33(6)	83.99(7)	81.17(7)	102.1(2)	126.3(1)	p
26	84.58(7)	79.70(6)	80.29(6)	81.09(6)	102.4(2)	118.0(1)	p

[a] Cf. footnotes a and b of Table 5. [b] Bridging rhomb. [c] Six-membered ring. [d] Dihedral angle. [e] p = planar, t = (distorted) tetrahedral.

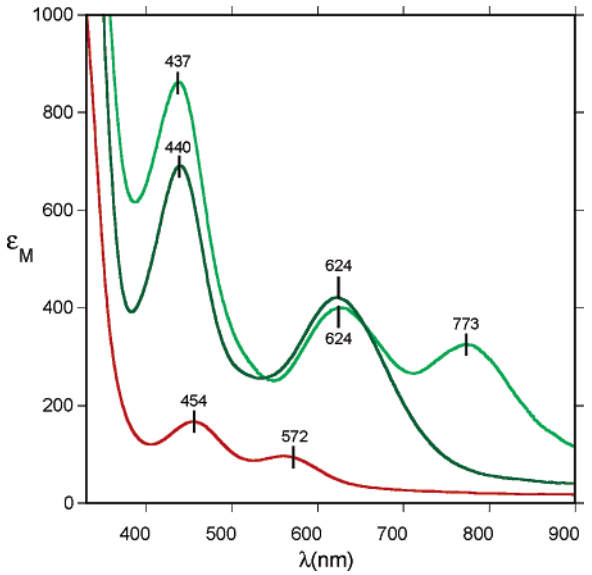

Figure 9. Visible absorption spectra of $[Ni(L\text{-}655)]^{2-}$ (**24**, red), $[\{Ni(L\text{-}655)\}_2Ni]^{2-}$ (**23**, dark green), and $[\{Ni(L\text{-}655)\}_2Cu]^{2-}$ (**27**, light green) in acetonitrile solutions; band maxima are indicated.

Reaction of **22g** with 1 equiv of $Ni(OAc)_2$ and 4 equiv of NaOMe in methanol resulted in the formation of trinuclear green $[\{Ni(L\text{-}655)\}_2Ni]^{2-}$ (**23**), derived from the tetradeprotonated ligand and isolated in 44% yield as the Et_4N^+ salt. The desired mononuclear complex, red $[Ni(L\text{-}655)]^{2-}$ (**24**), was obtained in 79% yield by bridge cleavage of **23** with 4 equiv of NaOMe and 1 equiv of ligand **22g** in methanol. The two complexes, which are easily distinguished by the absorption spectra in Figure 9, are readily interconverted. Treatment of **24** with 1 equiv of $[Ni(PR_3)_2Cl_2]$ (R = Me, Ph) in acetonitrile quickly generated **23**. Reaction of **23** with 4 equiv of $(Et_4N)(CN)$ in acetonitrile immediately afforded **24**. Reaction products, including $(Et_4N)_2[Ni(CN)_4]$, were isolated in nearly quantitative yield and were identified by X-ray diffraction.

Complex **23** is centrosymmetric such that the Ni(L-655) portions are transoid (Figure 7). The coordination unit is approximately planar; deviations from the $Ni-S_2N_2$ least-squares plane are appreciable for Ni1 (0.098(3) Å), N1 (0.053(4) Å), and S2 (0.050(3) Å). Reaction of 2 equiv of $[Ni(L\text{-}655)]^{2-}$ with 1 equiv of $Cu(OTf)_2$ in acetonitrile afforded trinuclear centrosymmetric $[\{Ni(L\text{-}655)\}_2Cu]^{2-}$ (**27**, Figure 8), essentially isostructural with **23**. Dimensions of the bridging rhombs in the two complexes are nearly identical (Tables 5 and 6). Nickel(II) complexes containing the central portion $Ni_3(\mu_2\text{-}SR)_4$, and nonplanar bridging rhombs with Ni−Ni separations in the range 2.6−3.2 Å, are well established.[15,24,50−55]

Considerable interest attends the structure of mononuclear **24** (Figure 7) as an unconstrained analogue of the Ni^{II}(Cys-Gly-Cys) sites in A-clusters, which have not yet been defined in an X-ray structure with better than 1.9 Å resolution.[8,9] The complex has an exactly planar coordination sphere and one planar five-membered ring containing atoms C3 and C4. The two other chelate rings are puckered. Atom C1 in the five-membered ring is displaced 0.51 Å from the $Ni-S_2N_2$ plane while in the six-membered ring atoms C6 and C7 are removed by 0.12 and 0.38 Å on opposite sides of this plane. As expected, the bite angle in the five-membered ring (89.05(6)°) is considerably smaller than that in the more flexible six-membered ring (102.0(5)°), where the Ni−N distance is 0.09 Å shorter. Dimensions are similar to those of the 6−5−6 Ni^{II} diamidodithiolate complex of Linck et al.[15] While no detailed comparison can yet be made, Ni−S distances and S−Ni−S angles of A-clusters calculated from X-ray coordinates (Tables 5 and 6) are credibly near those of **24**. This is also the case for Ni−S = 2.19−2.20 Å and Ni−N/O = 1.87−1.89 Å for the planar sites in *M. thermoacetica* CODH[56] and *M. thermophilia* decarbonylase/

(50) Wei, C. H.; Dahl, L. F. *Inorg. Chem.* **1970**, *9*, 1878−1887.
(51) Barrera, H.; Suades, J.; Perucaud, M. C.; Briansó, J. L. *Polyhedron* **1984**, *3*, 839−843.
(52) Turner, M. A.; Driessen, W. L.; Reedijk, J. *Inorg. Chem.* **1990**, *29*, 3331−3335.
(53) Farmer, P. J.; Solouki, T.; Mills, D. K.; Soma, T.; Russell, D. H.; Reibenspies, J. H.; Darensbourg, M. Y. *J. Am. Chem. Soc.* **1992**, *114*, 4601−4605.
(54) Golden, M. L.; Jeffery, S. P.; Miller, M. L.; Reibenspies, J. H.; Darensbourg, M. Y. *Eur. J. Inorg. Chem.* **2004**, 231−236.
(55) Hatlevik, O.; Blanksma, M. C.; Mathrubootham, V.; Arif, A. M.; Hegg, E. L. *J. Biol. Inorg. Chem.* **2004**, *9*, 238−246.
(56) Russell, W. K.; Stålhandske, C. M. V.; Xia, J.; Scott, R. A.; Lindahl, P. A. *J. Am. Chem. Soc.* **1998**, *120*, 7502−7510.
(57) Chalbot, M.-C.; Mills, A. M.; Spek, A. L.; Long, G. L.; Bouwman, E. *Eur. J. Inorg. Chem.* **2003**, 453−457.
(58) Lai, C.-H.; Reibenspies, J. H.; Darensbourg, M. Y. *Angew. Chem., Int. Ed. Engl.* **1996**, *35*, 2390−2393.
(59) Drew, M. G. B.; Rice, D. A.; Richards, K. M. *J. Chem. Soc., Dalton Trans.* **1980**, 2075−2080.
(60) Musie, G.; Farmer, P. J.; Tuntulani, T.; Reibenspies, J. H.; Darensbourg, M. Y. *Inorg. Chem.* **1996**, *35*, 2176−2183.
(61) Harrop, T. C.; Olmstead, M. M.; Mascharak, P. K. *Inorg. Chim. Acta* **2002**, *338*, 189−195.
(62) Mills, D. K.; Hsiao, Y. M.; Farmer, P. J.; Atnip, E. V.; Reibenspies, J. H.; Darensbourg, M. Y. *J. Am. Chem. Soc.* **1991**, *113*, 1421−1423.
(63) Colpas, G. J.; Day, R. O.; Maroney, M. J. *Inorg. Chem.* **1992**, *31*, 5053−5055.
(64) Fox, S.; Stibrany, R. T.; Potenza, J. A.; Schugar, H. J. *Acta Crystallogr., Sect. C: Cryst. Struct. Commun.* **1996**, *52*, 2731−2734.
(65) Miller, M. L.; Ibrahim, S. A.; Golden, M. L.; Darensbourg, M. Y. *Inorg. Chem.* **2003**, *42*, 2999−3007.
(66) Amoroso, A. J.; Chung, S. S. M.; Spencer, D. J. E.; Danks, J. P.; Glenny, M. W.; Blake, A. J.; Cooke, P. A.; Wilson, C.; Schröder, M. *Chem. Commun.* **2003**, 2020−2021.

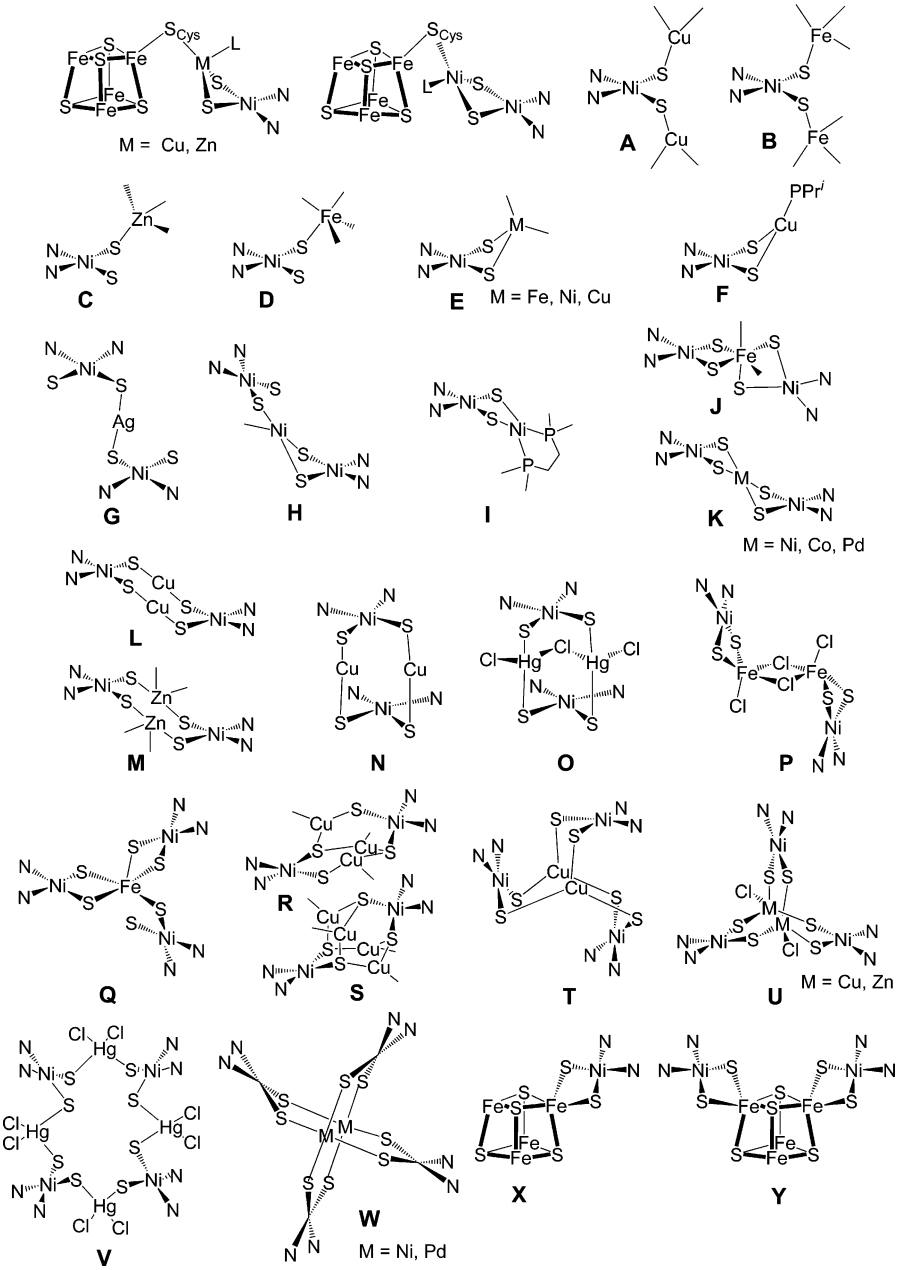

Figure 10. Depictions of structurally proven types of μ_2-S bridging modes (**A**−**Y**) based on the *cis*-$Ni^{II}S_2N_2$ coordination unit and taken from this work and literature reports (* = this work): ***A**, **B**,[57] ***C**, **D**,[58] **E**,[14,15] **F**,[15] ***G**, ***H**, ***I**,[17] ***K**,[50−55,59−61] **L**,[15] ***M**, ***N**,[14] ***O**, **P**,[62] **Q**,[63] **R**,[64] **S**,[65] ***T**,[14,66] **U**,[43] ***V**, **W**,[54,55,66,67] **X**,[19] **Y**.[19,20] Also shown are bridging modes of the CODH/ACS A-clusters (first row).

synthase.[12] Complex **23** shows an irreversible oxidation in DMF with $E_{pc} = -0.32$ V, similar to the behavior of **1** and related complexes at a lower temperature where dimerization of the generated Ni^{III} monoanion is likely.[30]

In addition to trinuclear **23** and **27**, bridged dinuclear neutral complexes, red **25** and red-brown **26**, were prepared by the reaction of **24** with Ni^{II} diphosphine complexes (Scheme 6). These molecules include a planar $Ni-P_2S_2$ unit and one nonplanar $Ni_2(\mu_2\text{-}S)_2$ bridging rhomb of similar dimensions (Figure 8, Tables 5 and 6). Dinuclear complexes containing the structural element $Ni^{II}(\mu_2\text{-}SR)_2Ni^{II}$ are not uncommon (see below), a related example being a neutral (dppe)Ni($Ni-S_2N_2$) species derived from a complex with a 5−6−5 ring pattern.[17] The same bridge type is present in a $(OC)_2Ni(Ni-S_2N_2)$ complex[15] in which, however, the bridge rhomb $Ni^0(\mu_2\text{-}S)_2Ni^{II}$ is in a different oxidation state. After this work was completed, Krishnan and Riordan[18] reported mononuclear and trinuclear 6−5−5 Ni^{II} complexes of O,N-protected Cys-Gly-Cys, and two diphosphine derivatives of the mononuclear complex that contain $Ni_2(\mu_2\text{-}S)_2$ rhombs. Structures were not determined.

Library of Ni−S Bridging Modes of $Ni^{II}-S_2N_2$ Fragments. At this point, we summarize the known bridging interactions of complexes with cis-planar $Ni^{II}-S_2N_2$ coordination units. The collection **A**−**Y**, set out in Figure 10, includes structurally established examples from this and other

(67) Konno, T.; Yonenobu, K.; Hidaka, J.; Okamoto, K. *Inorg. Chem.* **1994**, *33*, 861−864.
(68) Schneider, J.; Hauptmann, R.; Osterloh, F.; Henkel, G. *Acta Crystallogr., Sect. C: Cryst. Struct. Commun.* **1999**, *55*, 328−330.

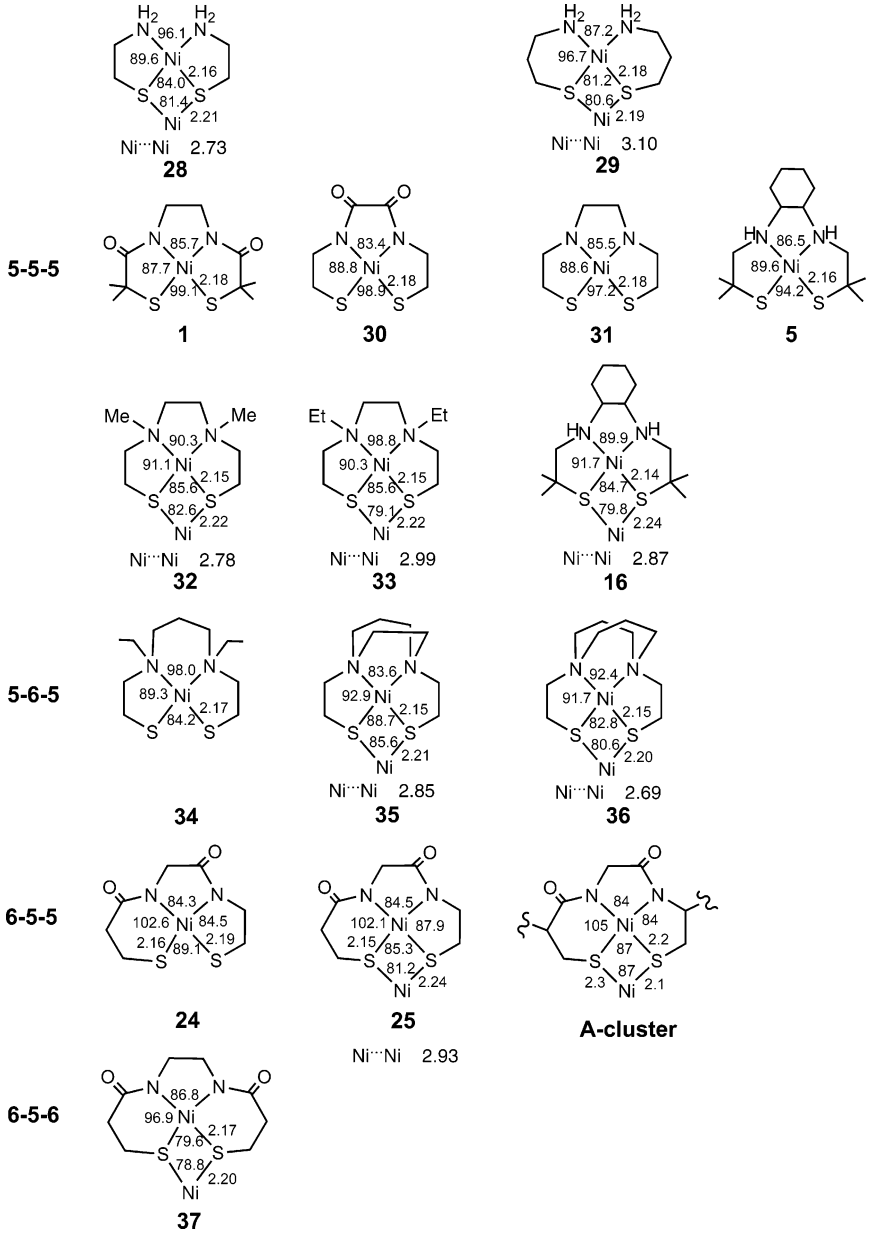

Figure 11. Schematic structures of the $Ni^{II}-S_2N_2$ complexes and those containing the $Ni_2(\mu_2\text{-}S)_2$ rhombic bridging unit **K** (Figure 10), showing selected (mean) angles (deg) and distances (Å). All known structure types are included. Complexes **1**, **5**, **16**, **24**, and **25** are from this work; see the appropriate references for **28**,[50] **29**,[51] **30**,[55] **31**,[55] **32**,[52] **33**,[17] **34**,[68] **35**,[54] **36**,[53] **37**.[55]

work already cited, and all additional cases. The bridging modes divide broadly into two types, nonrhombic Ni−(μ_2-SR)−M and rhombic Ni−(μ_2-SR)$_2$−M. The first type can be distributed into five classes: Ni−(μ_2-SR)−ML_n, in which atom M has no other bridging interaction (**A**−**D**); Ni−(μ_2-SR)−M−(μ_2-SR)$_n$, in which atom M has one (n = 1, **G**, **L**−**N, O**, **R**, **V**), two (n = 2, **H**, **T**, **U**), three (n = 3, **W**), or four (n = 4, **Q**) additional bridging interactions. Rhombic bridge structures are known with M = Fe^{II} (**E**, **J**, **P**, **Q**, **X**, **Y**), Co^{II} (**K**), Ni^{II} (**E**, **H**, **I**, **K**), Cu^{I} (**E**, **F**), and Pd^{II} (**K**). This classification serves to emphasize the diversity of nonrhombic bridging modes. Note the occurrence of one Ni−(μ_2-SR)−Fe bridge to a single iron atom (**B**, **D**). Rhombic interactions are not uncommon and sustain double bridges to iron atoms alone (**E**, **P**, **Q**) or integrated into an Fe_4S_4 cluster (**X**, **Y**). While these interactions are with distal nickel site representations, their existence suggests the feasibility of thiolate bridging of a proximal site analogue to a cluster iron atom, a matter relevant to step iii of analogue construction.

With nickel being established as the catalytic metal in the proximal site, the $Ni_2(\mu_2\text{-}S)_2$ rhombic bridging modes **H**, **I**, and **K** (M = Ni) assume particular significance. We offer some observations on bridging interactions with the aid of Figure 11, which includes selected parameters of cis-planar $Ni^{II}-S_2N_2$ molecules and some nine synthetic bridged derivatives organized according to the chelate ring pattern. Additional structural data are found in Tables 3−6. Bis-chelate complexes **28** and **29** reflect structural parameters

that are unconstrained by a covalent N,N-linkage between five- and six-membered chelate rings, respectively.

We note certain structural aspects, with due recognition that some examples are limited in number and there are occasional exceptions (e.g., **18** and **19**, Tables 3 and 4). (i) Chelate ring (2.14−2.19 Å) and bridging (2.19−2.24 Å) Ni−S bond distances show little variation with ring size. Certain other parameters are variable. (ii) Two-carbon bridges in the 5−5−5 and 5−6−5 series decrease the N−Ni−N bite angle below the unconstrained value of 96.1° (**28**), except for **33** and **34** which are slightly above this value. (iii) N−Ni−S bite angles vary little in the 5−5−5 and 5−6−5 series (87.7−92.9°) and bracket the unconstrained value of 89.6°. (iii) N−Ni−S bite angles in the 6−5−5 and 6−5−6 series (96.9−102.6°, limited data) are the same or slightly above the unconstrained value of 96.7° (**29**). (iv) In unbridged species, S−Ni−S bite angles are variable and decrease in the order 5−5−5 > 6−5−5 > 5−6−5. The larger angles are associated with the more rigid molecules having three five-membered rings. (v) In the 5−5−5 series, bridge formation requires tightening of the angles in iv by ca. 10−14°; much smaller adjustments (0.5°) are necessary in the 5−6−5 and 6−5−5 series. (vi) The S−Ni−S and Ni−S−Ni (not given) angles and the two types of Ni−S distances in the bridging rhombs conform closely to the values in the appropriate bridged species **28** or **29**. (vii) With larger and more thiophilic Cu^{I}, bridging in the 5−5−5 series requires no significant change in angle (Table 4). Under the scenario in which the A-cluster distal site is formed first, followed by insertion of the proximal metal atom, the Ni(Cys-Gly-Cys) 6−5−5 ring pattern is appropriately devised to bind Ni^{II} or Cu^{I} with minimal structural reorganization within the chelate structure.

Summary

This investigation provides synthetic routes to and structures of an expanded set of bridging modes between three structurally defined cis-planar $Ni^{II}-S_2N_2$ template complexes (**1**, **5**, **24**) and various Ni^{II}, Zn^{II}, $Cu^{I,II}$, Ag^{I}, and Hg^{II} reactants. One of these complexes (**24**) reproduces the 6−5−5 chelate ring pattern of the distal Ni^{II} site of the A-cluster of CODH/ACS. Certain of the bridging interactions, summarized as **A**−**Y** (Figure 10), have not been previously demonstrated in any context. The most frequently encountered bridging modes are the nonplanar $Ni^{II}(\mu_2\text{-SR})_2M$ rhombs with M = Ni^{II} (planar) and Cu^{I} (tetrahedral) dimensionally similar to those encountered in the enzyme sites. Here, the chelated and bridging nickel atoms simulate the distal and proximal sites, respectively, of the A-clusters, as in the complexes [{Ni(L-655)}Ni($R_2PCH_2CH_2PR_2$)] (**25**, **26**). Note also the $Ni_2(\mu_2\text{-S})_2$ unit in **19**, where a proximal-like Ni^{II} atom forms thiolate bridges to another metal, similar to one of the proximal site bridges in the A-cluster. This work, and that of others,[15,17,18] addresses steps i and ii in the construction of an A-cluster analogue with two nickel sites. Our current research is directed toward step iii, the formation of thiolate bridges $Ni^{II}-(\mu_2\text{-SR})-Fe_4S_4$ between the proximal nickel atom and the cluster.

Acknowledgment. This research was supported by NIH Grant GM 28856.

Supporting Information Available: X-ray crystallographic files in CIF format for the structure determinations of the twenty-four compounds in Tables 1 and 2; spectroscopic data for compound **22g** and complexes **23** and **24**. This material is available free of charge via the Internet at http://pubs.acs.org.

IC040055S